AWARD NUMBER: W81XWH-18-1-0162

TITLE: Modeling the Impact of Radiation Protectors on Radiation-induced Sarcoma Risk

PRINCIPAL INVESTIGATOR: David G. Kirsch, MD, PhD

CONTRACTING ORGANIZATION: Duke University
Durham, NC 27705

REPORT DATE: August 2019

TYPE OF REPORT: Annual

PREPARED FOR: U.S. Army Medical Research and Materiel Command
Fort Detrick, Maryland 21702-5012

REPORT DOCUMENTATION PAGE

Form Approved
OMB No. 0704-0188

1. REPORT DATE *(DD-MM-YYYY)*	2. REPORT TYPE	3. DATES COVERED *(From - To)*
August 2019	Annual	1 Aug 2018 - 31 Jul 2019

4. TITLE AND SUBTITLE

Modeling the Impact of Radiation Protectors on Radiation-Induced Sarcoma Risk

5a. CONTRACT NUMBER

5b. GRANT NUMBER
W81XWH-18-1-0162

5c. PROGRAM ELEMENT NUMBER

6. AUTHOR(S) David G. Kirsch, Andrea R. Daniel

5d. PROJECT NUMBER

5e. TASK NUMBER

5f. WORK UNIT NUMBER

7. PERFORMING ORGANIZATION NAME(S) AND ADDRESS(ES)

8. PERFORMING ORGANIZATION REPORT NUMBER

9. SPONSORING / MONITORING AGENCY NAME(S) AND ADDRESS(ES)
U. S. Army Medical Research and Material Command
Fort Detrick, MD 21702-5012

10. SPONSOR/MONITOR'S ACRONYM(S)

11. SPONSOR/MONITOR'S REPORT NUMBER(S)

12. DISTRIBUTION / AVAILABILITY STATEMENT

Approved for Public Release; Distribution Unlimited

13. SUPPLEMENTARY NOTES

14. ABSTRACT

The threat of a radiation disaster, such as a nuclear accident or terrorist attack, is a growing concern for the military and warrants the development of medical countermeasures to prevent and mitigate acute and delayed radiation injury. We will evaluate the risks of delayed radiation-induced carcinogenesis after radiation alone or in a setting that models radiation protection strategies that block p53-dependent cell death pathways. To reduce radiation-induced cancer risk and to steer development of rationally designed pharmacological agents to mitigate radiation injury, we aim to elucidate the biological drivers of radiation-induced late effects. Understanding the link between improved survival of irradiated cells and cancer development will aid in selecting pharmacological strategies that not only prevent acute radiation injury, but also do not increase radiation carcinogenesis, thus improving outcomes for soldiers exposed to radiation.

15. SUBJECT TERMS
sarcoma, acute radiation syndrome, p53, satellite cells, radiation carcinogenesis, countermeasures, cancer, tumor, radiation injury, tumor suppressor

16. SECURITY CLASSIFICATION OF:			17. LIMITATION OF ABSTRACT	18. NUMBER OF PAGES	19a. NAME OF RESPONSIBLE PERSON
a. REPORT	b. ABSTRACT	c. THIS PAGE			19b. TELEPHONE NUMBER *(include area code)*
U	U	U	UU		USAMRMC

TABLE OF CONTENTS

1. **INTRODUCTION:** *Narrative that briefly (one paragraph) describes the subject, purpose and scope of the research.*

The threat of a radiation disaster, such as a nuclear accident or terrorist attack, is a growing concern for the military and warrants the development of medical countermeasures to prevent and mitigate acute and delayed radiation injury. We will evaluate the risks of delayed radiation-induced carcinogenesis after radiation alone or in a setting that models radiation protection strategies that block p53-dependent cell death pathways. To reduce radiation-induced cancer risk and to steer development of rationally designed pharmacological agents to mitigate radiation injury, we aim to elucidate the biological drivers of radiation-induced late effects. Understanding the link between improved survival of irradiated cells and cancer development will aid in selecting pharmacological strategies that not only prevent acute radiation injury, but also do not increase radiation carcinogenesis, thus improving outcomes for soldiers exposed to radiation. We hypothesize that blocking cell death in irradiated tissues will increase survival of mice exposed to radiation, but damaged cells that would have died will develop into cancers like sarcomas. Late effects of radiation include life-threatening sarcomas or other solid tumors. The overall goal of this proposal is to evaluate whether strategies to prevent acute radiation injury by blocking the death of irradiated cells alter the risk of subsequently developing late effects of radiation including sarcomas. We utilize mice with inducible p53 shRNA expression to temporarily knockdown p53 during left hind leg irradiation compared to littermate controls. Mice are followed for tumor development and evaluated for mechanistic studies, which includes assessing cell fate of muscle satellite cells after radiation and p53 transcriptional programs.

2. **KEYWORDS:** *Provide a brief list of keywords (limit to 20 words).*

sarcoma, acute radiation syndrome, p53, satellite cells, radiation carcinogenesis, countermeasures, cancer, tumor, radiation injury, tumor suppressor

3. **ACCOMPLISHMENTS:** *The PI is reminded that the recipient organization is required to obtain prior written approval from the awarding agency grants official whenever there are significant changes in the project or its direction.*

What were the major goals of the project?
List the major goals of the project as stated in the approved SOW. If the application listed milestones/target dates for important activities or phases of the project, identify these dates and show actual completion dates or the percentage of completion.

Specific Aims

1. Determine the effect of blocking p53-induced cell death on radiation-induced sarcoma.
   1.1 Evaluate the effect of blocking p53 on hind limb sarcoma development in irradiated mice
   1.2 Examine the genetic mechanisms by which radiation promotes sarcomagenesis

2. Dissect the mechanisms of radiation-induced sarcoma development by examining p53-dependent satellite cell fate following irradiation.

2.1 Test whether transient knockdown of p53 protects muscle stem (satellite) cells from radiation induced death
2.2 Determine if radiation induces a selective advantage for the outgrowth of preexisting p53 mutant tumor-initiating satellite cells
2.3 Examine the specific p53 mediated transcriptional programs necessary for tumor suppression of radiation-induced sarcoma

Major Task 1 (Aim 1)

The first major goal for task 1 is evaluating the effect of blocking p53 on hind limb sarcoma development in irradiated mice (Aim 1.1). We have followed the first cohorts of mice for sarcoma development for this task and the results are described below. We are analyzing the radiation induced injury data from these mice and preliminary results are described below. Additional C3H cohorts of mice remain under evaluation to complete this task.

The second major goal for task 1 was to examine the genetic mechanisms by which radiation promotes sarcomagenesis by using whole exome sequencing of tumor and paired normal tissues (Aim 1.2). We have successfully completed this goal, which resulted in a recent publication (Lee, Mowery, Daniel, et al., *JCI Insight* 2019). Notably, we hypothesized that radiation-induced tumors would exhibit a common genetic signature and specific recurring mutations that drive sarcomagenesis. While we did identify a genetic signature for radiation-induced tumors, no specific driver mutations were found. Therefore, we hypothesize that radiation-induced sarcomas may be driven by transcriptional mechanisms regulating RNA expression rather than driver mutations in the DNA. Therefore, we have submitted radiation-induced sarcoma samples for RNA sequencing to further explore this hypothesis and complete this task.

Major Task 2 (Aim 2)

The first major goal for task 2 is to test whether transient knockdown of p53 protects muscle stem (satellite) cells from radiation induced death (Aim 2.1). We have initiated these studies and established a reliable protocol for isolating and quantifying muscle stem cells. Our preliminary data suggests that temporary knockdown of p53 in mice does increase muscle stem cell survival after high dose irradiation. Experiments to further address this question are currently ongoing.

The second major goal for task 2 is to determine if radiation induces a selective advantage for the outgrowth of preexisting p53 mutant tumor-initiating satellite cells (Aim 2.2). These experiments were designed to address the hypothesis that the mechanism of radiation-induced sarcoma development in the setting of temporarily reduced p53 would be similar to our prior studies in radiation-induced thymic lymphoma development (Lee et al., Nature Communications 2015). In particular, we hypothesized that like thymic lymphomas, sarcomas would develop after radiation in a non-cell autonomous manner. In radiation-induced thymic lymphomas, irradiated bone marrow cells with decreased p53 survive radiation insult and function to prevent the development of lymphoma by competing with preexisting tumor initiating cells. In contrast, bone marrow cells with wild type p53 levels die by radiation-induced apoptosis, which allows preexisting tumor initiating cells to expand into the niche free of competition and form a lymphoma. Importantly, evidence from our studies in Task 1 indicates that radiation-induced sarcomas do not develop in a similar manner to radiation-induced thymic lymphomas. Instead, results from Task 1 support an alternative model of a

cell autonomous mechanism for radiation-induced sarcomas. Specifically, while temporary p53 knockdown prevents radiation-induced thymic lymphoma development, we find that temporary p53 knockdown increases radiation-induced sarcoma development. Furthermore, using whole exome sequencing, we identified a strong oxidative mutation genetic signature in the radiation-induced sarcomas (Lee, Mowery, Daniel, et al., *JCI Insight* 2019). These data taken together indicate a cell autonomous mechanism whereby muscle stem cells with low p53 levels undergo radiation mediated genetic damage, but do not undergo apoptosis. Thus, our revised working model is that damaged muscle stem cells survive radiation insult and go on to form a sarcoma, which is strongly supported by data generated in Task 1. Thus, as this sub-aim was designed to test a model in Task 2 that is no longer supported by the available data, we did not initiate this experiment and we hereby request permission to remove this experiment from our statement of work and milestones.

The third major goal of Task 2 is to examine the specific p53 mediated transcriptional programs necessary for tumor suppression of radiation-induced sarcoma (Aim 2.3). We initially proposed to use *Pax7CreER; p53$^{LSL\text{-}25,\ 26/FL}$* and *Pax7-CreER; p53$^{LSL\text{-}25,26,\ 53,\ 54/FL}$* mice with littermate control mice to address this question. However, as we started this experiment we realized that utilizing Myf6Cre mice instead of Pax7CreER mice would allow us to complete the task with a higher chance of success because Myf6 is expressed early in embryonic development in cells whose progeny become all of the muscle stem cells so that Cre recombines target genes in all of the muscle stem cells in all Myf6Cre mice, while tamoxifen activates CreER in a different number of muscle stem cells in different Pax7CreER mice. Therefore, using Myf6Cre to drive p53 mutation in muscle stem cells will generate a uniform cohort of mice to study the impact of p53 mutation in muscle stem cells on radiation-induced sarcomagenesis. Because radiation-induced sarcomagenesis occurs in only 20-25% of the experimental mice in Aim 1.1 (see Figure 1 A-B, below), using Myf6Cre instead of the tamoxifen inducible Pax7CreER will ensure that variable tamoxifen distribution to activate p53 mutation in the muscle stem cells does not decrease the statistical power for this experiment. Therefore, we request to substitute Myf6Cre for Pax7CreER for the proposed experiment for Task 2. Once we receive approval for this change, we will generate the *Myf6Cre; p53$^{LSL\text{-}25,\ 26/FL}$* and *Myf6Cre; p53$^{LSL\text{-}25,26,\ 53,\ 54/FL}$* mice with littermate control mice for this sub-aim of Task 2.

What was accomplished under these goals?

For this reporting period describe: 1) major activities; 2) specific objectives; 3) significant results or key outcomes, including major findings, developments, or conclusions (both positive and negative); and/or 4) other achievements. Include a discussion of stated goals not met. Description shall include pertinent data and graphs in sufficient detail to explain any significant results achieved. A succinct description of the methodology used shall be provided. As the project progresses to completion, the emphasis in reporting in this section should shift from reporting activities to reporting accomplishments.

1) Major activity (Aim 1)

We irradiated *Actin-rtTA; TRE-p53.1224* and littermate control mouse cohorts on a C3H and C57Bl/6J mixed genetic background. 3 to 4-month-old male and female mice were placed on a doxycycline (Dox) containing diet for 10 days to knockdown p53 prior to delivery of 30 Gy or 40 Gy to the left hind limb using a micro-irradiator (225 kVp X-rays). Following irradiation, mice were placed on standard chow. Mice were examined weekly for signs of tumors. Once tumors developed,

they were harvested for histological and molecular characterization. In addition, normal (liver, muscle) tissues was banked for future whole exome and RNA sequencing experiments as a germline/normal comparison for the radiation-induced sarcomas. We also continue to follow the *CMV-rtTA; TRE-p53.1224* C3H background or littermate control cohorts that received a single dose of 30 Gy left hind limb irradiation. We are also following additional control cohorts of unirradiated *Actin-rtTA* or *CMV-rtTA; TRE-p53.1224* and littermate control mice (n=30 per sex per genotype) and irradiated mice that were not fed Dox diet. Log-rank test will be used to perform statistical analysis on the data as previously described.

To determine the histological subtypes of radiation-induced sarcomas that developed in the mice we used formalin fixed paraffin embedded samples. Sections from each tumor were stained with specific antibodies against known markers for tumor characterization (Table 1). Analysis of the stained slides is currently ongoing.

Table 1

Antibody/Stain	**Purpose**
S100	Rule out melanoma
Smooth Muscle Actin	Positive in Leiomyosarcoma
MyoD	Myogenic UPS
Myogenin	Negative in UPS, positive in embryonic Rhabdomyosarcoma (RMS)
Pax7	Satellite cell marker, promotes metastasis
Cyokeratin 5	Rule out carcinoma
CD45	Rule out lymphoma
Desmin	Positive in Embryonic RMS
CD31	Positive in Angiosarcoma
hematoxylin and eosin	Basic histology and cytology

2 to 4) Specific objective, results, and conclusions (Aim 1.1 Evaluate the effect of blocking p53 on hind limb sarcoma development in irradiated mice)

To address whether improving survival of irradiated cells by temporarily reducing p53 levels increases radiation-induced solid tumors, we examined radiation-induced sarcoma development in the setting of temporary p53 knockdown. Our data show that mice with all the genetic components to achieve temporary p53 knockdown while on the Dox diet exhibited an increased incidence of radiation-induced sarcoma development compared to control mice. Indeed, 20% of temporary p53 knockdown animals that received 30 Gy to the left hind limb developed a sarcoma in the radiation field compared to 2% of control animals (Figure 1A). Likewise, 25% of the temporary p53 knockdown animals that received 40 Gy developed an in-field sarcoma whereas only 4% of the control mice developed left hind limb sarcomas (Figure 1B). These data demonstrate that temporary p53 knockdown increases the risk of sarcoma development following single-dose irradiation.

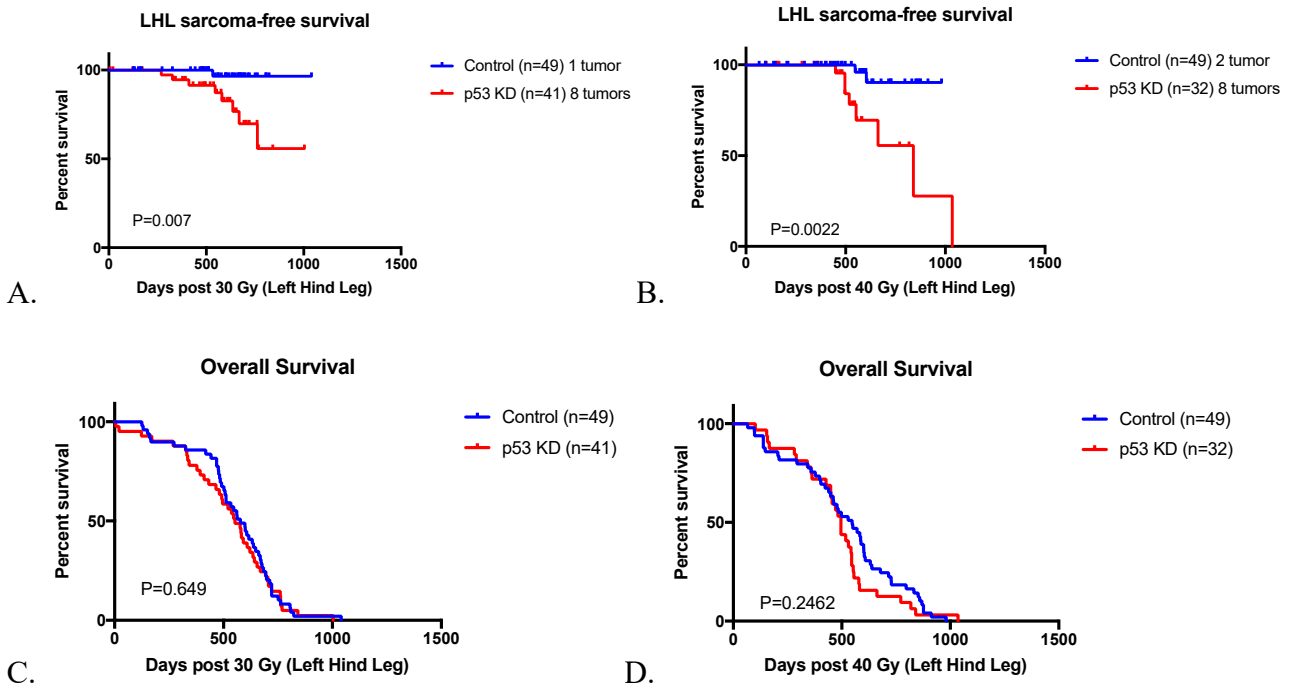

Figure 1. A. Kaplan-Meier curves showing left hind limb (LHL) sarcoma-free survival of *Actin-rtTA; TRE-p53.1224* (p53 knockdown or p53 KD) mice compared to littermate controls after 30 Gy left hind limb irradiation. B. Kaplan-Meier curves showing LHL sarcoma-free survival of *Actin-rtTA; TRE-p53.1224* (p53 KD) mice compared to littermate controls after 40 Gy irradiation. C. Kaplan-Meier curves showing overall survival of *Actin-rtTA; TRE-p53.1224* (p53 KD) mice compared to littermate controls after 30 Gy LHL irradiation. D. Kaplan-Meier curves showing overall survival of *Actin-rtTA; TRE-p53.1224* (p53 KD) mice compared to littermate controls after 40 Gy LHL irradiation. Log-rank test was used to generate p values.

We have previously shown that muscle tissue injury and wounds promote sarcoma development (Van Mater et al. *Cancer Research*, 2015). Radiation-induced chronic wounds may occur due to an acute wound that fails to heal or may arise months to years after radiation exposure in tissue that initially appears to have recovered from acute toxicity. Late persistent wounds are characterized by inflammation, ulceration, fibrosis, or necrosis of soft tissue, cartilage and bone. Damage to the vasculature of irradiated tissues may contribute to impaired wound healing due to a lack of neovascularization and thus insufficient perfusion. The cohorts of irradiated (and unirradiated control) mice were followed for the development of acute and late wounds by scoring the level of tissue injury on a weekly basis. Mice were evaluated based on a previously published rubric for skin injury that we adapted to comprehensively assess radiation-induced normal tissue toxicity of the skin, bone, and muscle (Douglas et al. *Radiation Researc*h, 1976). Mice exhibiting signs of injury (skin breakdown and/or swelling) were given a score of 1 and scoring increases with severity to a score of 4, or loss of the foot. Temporarily reducing p53 expression increases the number of mice that sustain a wound following single high dose left hind limb irradiation at 30 or 40 Gy (Figure 2A-B). However, the overall average peak score (the highest injury score the mouse received during weekly scoring after irradiation) was not significantly different among control and *Actin-rtTA; TRE-p53.1224* animals. Interestingly, while on average 75% of the total mice irradiated, regardless of genotype or dose of radiation, exhibited an injury (scored above a 1), 95% of the mice that developed left hind limb

sarcomas exhibited injuries. Notably, the average peak injury score for tumor bearing mice was 3.54 while the average peak injury score for all irradiated mice was 2.28. These data suggest that radiation-induced injury may play a stimulatory role in sarcoma development. Further analysis of this data set is underway.

A.

30 Gy Percent Injured			
	Total	Injured	Percentage
Control	49	35	71%
p53KD	41	35	85%
			p>0.05

B.

40 Gy percent injured			
	Total	Injured	Percentage
Control	45	30	67%
p53KD	31	23	74%
			p>0.05

C. D.

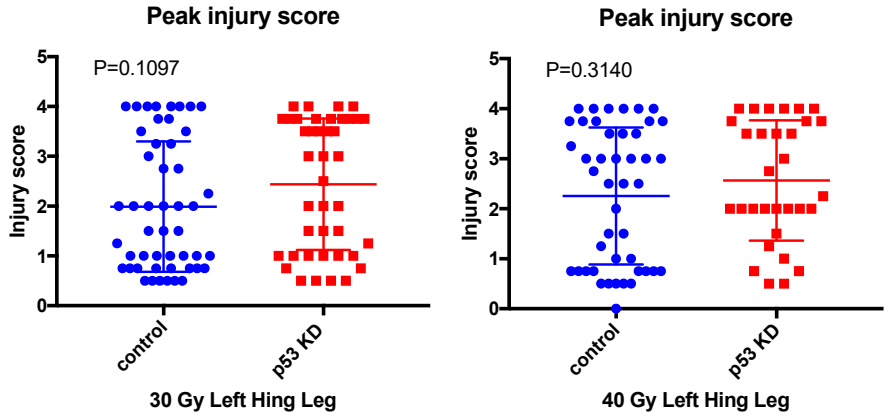

Figure 2. A. Percent of control or of *Actin-rtTA; TRE-p53.1224* (p53KD) mice with an injury score greater than 1 after 30 Gy left hind limb irradiation. B. Percent of control or of *Actin-rtTA; TRE-p53.1224* (p53KD) mice that with an injury score greater than 1 after 40 Gy left hind limb irradiation. P value calculated using Chi Square tests. C. The peak injury scores of control or of *Actin-rtTA; TRE-p53.1224* (p53KD) mice following 30 Gy left hind limb irradiation. D. The peak injury scores of control or of *Actin-rtTA; TRE-p53.1224* (p53KD) mice following 40 Gy left hind limb irradiation. P values are calculated using Students T-tests.

2 to 4) Specific objective, results, and conclusions (Aim 1.2 Examine the genetic mechanisms by which radiation promotes sarcomagenesis)

To identify mutational signatures specific to radiation-induced tumors and to gain insight into how distinct cell-intrinsic and -extrinsic factors affect cancer development within the same tissue type, we performed genomic analysis across murine soft-tissue sarcomas induced by mutagen, MCA,

oncogenic mutations, or ionizing radiation. Radiation-induced sarcomas were generated by focally irradiating the mouse hind limb using a single dose of 30 or 40 Gy. For comparison to radiation-induced sarcomas, we used an established genetically engineered mouse model of soft-tissue sarcoma in which localized delivery of Cre recombinase into the muscle of the hind limb activates oncogenic *Kras*^{G12D} and deletes both alleles of *p53* (Kirsch et al. *Nature Medicine,* 2007). In addition, we generated MCA-induced sarcomas in the hind limb of either WT or *p53*$^{fl/fl}$ mice in which both copies of *p53* were deleted by Cre recombinase. Using these mouse models of oncogene-driven, chemical carcinogen–induced, or radiation-induced soft-tissue sarcoma, we performed whole-exome sequencing (WES) on paired tumor and normal tissue from each mouse and observed distinct facultative molecular signatures that are specific to each carcinogenic driver. Remarkably, ionizing radiation produced tumors with relatively low levels of nonsynonymous mutations, but a high frequency of somatic copy number alterations, with a preponderance of deletions and a tendency toward C-to-T and G-to-A transitions. The results from this study were published in *JCI Insight*.

Lee CL*, Mowery YM*, Daniel AR*, Zhang D, Sibley AB, Delaney JR, Wisdom AJ, Qin X, Wang X, Caraballo I, Gresham J, Luo L, Van Mater D, Owzar K, Kirsch DG. Mutational landscape in genetically engineered, carcinogen-induced, and radiation-induced mouse sarcoma. *JCI Insight*. 2019 Jul 11;4(13). pii: 128698. doi: 10.1172/jci.insight.128698. PMID: 31112524. *equal contribution.

1) Major activity (Aim 2)

To explore the mechanism by which radiation-induced sarcomagenesis is altered with temporary p53 knockdown, we are examining the fate of muscle stem/progenitor (satellite) cells following irradiation. We are using *Pax7-nGFP* mice to identify and isolate Pax7-expressing satellite cells in order to examine whether muscle stem/progenitor cells are protected from radiation-induced cell death by p53 knockdown and whether surviving satellite cells compete with or become tumor-initiating cells during sarcoma development. We have established a protocol to examine surviving satellite cell fractions by flow cytometry on muscle (irradiated and unirradiated hind legs) harvested from *Pax7-nGFP*; *CMV-rtTA; TRE-p53.1224* and *Pax7-nGFP* control mice. Three to four-month-old male and female mice were placed on a dox containing diet for 10 days prior to delivery of 30 Gy to the left hind limb using a micro-irradiator (225 kVp X-rays). Following irradiation, mice were placed on standard chow and 48 hours later the leg muscles were harvested for analysis. The satellite cell isolation protocol was adapted from (Lui et al. Nature Protocols, 2015). Flow cytometry was performed to quantify the percentage of Pax7 positive, GFP expressing (satellite cells). These experiments are currently ongoing.

2 to 4) Specific objective, results, and conclusions (Aim 2)

The experiments for Aim 2.1 are in progress and the experiments for Aim 2.3 will commence once we have approval to switch Myf6Cre for Pax7CreER mice and when we generate the experimental mice from the breeding crosses.

What opportunities for training and professional development has the project provided?
If the project was not intended to provide training and professional development opportunities or there is nothing significant to report during this reporting period, state "Nothing to Report."

Describe opportunities for training and professional development provided to anyone who worked on the project or anyone who was involved in the activities supported by the project. "Training" activities are those in which individuals with advanced professional skills and experience assist others in attaining greater proficiency. Training activities may include, for example, courses or one-on-one work with a mentor. "Professional development" activities result in increased knowledge or skill in one's area of expertise and may include workshops, conferences, seminars, study groups, and individual study. Include participation in conferences, workshops, and seminars not listed under major activities.

The data from the radiation-induced sarcoma studies were analyzed in conjunction with data from other graduate student and postdoc projects studying other mouse models of sarcoma in the lab, which were supported by other funding sources. The data were combined for the manuscript published in *JCI Insight*. Trainees that worked on the combined publication increased their skills through data analysis, manuscript preparation and publication.

How were the results disseminated to communities of interest?
If there is nothing significant to report during this reporting period, state "Nothing to Report."

Describe how the results were disseminated to communities of interest. Include any outreach activities that were undertaken to reach members of communities who are not usually aware of these project activities, for the purpose of enhancing public understanding and increasing interest in learning and careers in science, technology, and the humanities.

Data from this project was the subject of a poster presentation for Andrea Daniel at the Duke University Radiation Oncology and Imaging Program annual retreat.

Data from this project was published in the following manuscript:

Lee CL*, Mowery YM*, Daniel AR*, Zhang D, Sibley AB, Delaney JR, Wisdom AJ, Qin X, Wang X, Caraballo I, Gresham J, Luo L, Van Mater D, Owzar K, Kirsch DG. Mutational landscape in genetically engineered, carcinogen-induced, and radiation-induced mouse sarcoma. *JCI Insight*. 2019 Jul 11;4(13). pii: 128698. doi: 10.1172/jci.insight.128698. PMID: 31112524. *equal contribution.

What do you plan to do during the next reporting period to accomplish the goals?
If this is the final report, state "Nothing to Report."

Describe briefly what you plan to do during the next reporting period to accomplish the goals and objectives.

For the Task 1 studies, we will continue to follow additional cohorts of irradiated and unirradiated control C3H mice for radiation-induced sarcoma development and injury. We will analyze RNA sequencing data from the mouse radiation-induced tumors. We will continue to score and analyze the

tumor histology slides to determine the histological subtypes of the mouse radiation-induced sarcomas.

For the Task 2 studies, we will use the satellite cell isolation protocol that we optimized to determine whether transient knockdown of p53 protects muscle stem (satellite) cells from radiation-induced cell death. In addition, we plan to breed p53 mutant mice with conditional expression in muscle stem cells using Myf6Cre. Once we have experimental mice with the appropriate genotype, we will irradiate the mice and follow them for sarcoma development.

4. **IMPACT:** D*escribe distinctive contributions, major accomplishments, innovations, successes, or any change in practice or behavior that has come about as a result of the project relative to:*

What was the impact on the development of the principal discipline(s) of the project?
If there is nothing significant to report during this reporting period, state "Nothing to Report."

Describe how findings, results, techniques that were developed or extended, or other products from the project made an impact or are likely to make an impact on the base of knowledge, theory, and research in the principal disciplinary field(s) of the project. Summarize using language that an intelligent lay audience can understand (Scientific American style).

Our *JCI Insight* manuscript represents a rigorous comparison of the genetic landscape of mouse sarcomas generated as a result of irradiation (funded by this project) or other distinct tumor initiating events (funded by other sources) within the same tissue type. By comparing the whole exome sequencing of radiation-induced sarcomas with other sarcomas, we defined a radiation-induced tumor genetic signature. In addition, the raw sequencing data from these studies has been deposited in a public repository for other researchers to access.

What was the impact on other disciplines?
If there is nothing significant to report during this reporting period, state "Nothing to Report."

Describe how the findings, results, or techniques that were developed or improved, or other products from the project made an impact or are likely to make an impact on other disciplines.

Nothing to Report

What was the impact on technology transfer?
If there is nothing significant to report during this reporting period, state "Nothing to Report."

Describe ways in which the project made an impact, or is likely to make an impact, on commercial technology or public use, including:

- *transfer of results to entities in government or industry;*
- *instances where the research has led to the initiation of a start-up company; or*
- *adoption of new practices.*

Nothing to Report

What was the impact on society beyond science and technology?
If there is nothing significant to report during this reporting period, state "Nothing to Report."

Describe how results from the project made an impact, or are likely to make an impact, beyond the bounds of science, engineering, and the academic world on areas such as:

- *improving public knowledge, attitudes, skills, and abilities;*
- *changing behavior, practices, decision making, policies (including regulatory policies), or social actions; or*
- *improving social, economic, civic, or environmental conditions.*

Nothing to Report

5. CHANGES/PROBLEMS: *The PD/PI is reminded that the recipient organization is required to obtain prior written approval from the awarding agency grants official whenever there are significant changes in the project or its direction. If not previously reported in writing, provide the following additional information or state, "Nothing to Report," if applicable:*

Changes in approach and reasons for change
Describe any changes in approach during the reporting period and reasons for these changes. Remember that significant changes in objectives and scope require prior approval of the agency.

Aim 1.2: The completion of this aim led to a new compelling hypothesis that changes in gene expression rather than recurrent gene mutations drive radiation-induced sarcomagenesis, which will now be explored by completing RNA sequencing analysis of the radiation-induced sarcomas. Please see the description of the rationale for this experiment in section 3 under the description of the activities for the second major goal of Task 1. The SOW was modified accordingly.

Aim 2.2: This sub-aim was designed to answer a question that is no longer relevant to our study because of new data generated supported a cell autonomous mechanism for radiation-induced sarcomagenesis. Therefore, this experiment was not been performed and we request to remove this experiment from the SOW. Please see the description of this rationale in section 3 under the description of the activities for the second major goal of Task 2. The SOW was modified accordingly.

Aim 2.3: In the proposed studies we described using Pax7CreER mice to drive the mutation of p53 in muscle stem cells after tamoxifen administration. However, we propose substituting Myf6Cre mice instead of Pax7CreER mice. Please see the scientific rationale for this change in section 3 under the description of the activities for the third major goal of Task 2. The SOW was modified accordingly.

Actual or anticipated problems or delays and actions or plans to resolve them
Describe problems or delays encountered during the reporting period and actions or plans to resolve them.

Aim 1.2: Because our initial hypothesis that radiation would cause recurrent mutations to cause sarcomas was not supported by the data in Task 1, we have added an RNA sequencing experiment to Aim 1.2 to test an alternative model where changes in gene expression after radiation drive

sarcomagenesis. Therefore, we have extended the timeline for completion of this aim. The SOW is modified accordingly.

Aim 2.3: Because we are now proposing Myf6Cre mice instead of Pax7CreER mice, the studies in Aim 2.3 have been delayed so that we can obtain permission for this change. Once permission for this change in experimental design is approved, we will begin to generate experimental mice and have modified the SOW accordingly.

Changes that had a significant impact on expenditures
Describe changes during the reporting period that may have had a significant impact on expenditures, for example, delays in hiring staff or favorable developments that enable meeting objectives at less cost than anticipated.

Nothing to Report

Significant changes in use or care of human subjects, vertebrate animals, biohazards, and/or select agents
Describe significant deviations, unexpected outcomes, or changes in approved protocols for the use or care of human subjects, vertebrate animals, biohazards, and/or select agents during the reporting period. If required, were these changes approved by the applicable institution committee (or equivalent) and reported to the agency? Also specify the applicable Institutional Review Board/Institutional Animal Care and Use Committee approval dates.

Significant changes in use or care of human subjects

Not Applicable

Significant changes in use or care of vertebrate animals

Nothing to Report

Significant changes in use of biohazards and/or select agents

Nothing to Report

6. **PRODUCTS:** *List any products resulting from the project during the reporting period. If there is nothing to report under a particular item, state "Nothing to Report."*

- **Publications, conference papers, and presentations**
  Report only the major publication(s) resulting from the work under this award.

  Journal publications. *List peer-reviewed articles or papers appearing in scientific, technical, or professional journals. Identify for each publication: Author(s); title; journal; volume: year; page numbers; status of publication (published; accepted, awaiting publication; submitted, under review; other); acknowledgement of federal support (yes/no).*

Lee CL*, Mowery YM*, Daniel AR*, Zhang D, Sibley AB, Delaney JR, Wisdom AJ, Qin X, Wang X, Caraballo I, Gresham J, Luo L, Van Mater D, Owzar K, Kirsch DG. Mutational landscape in genetically engineered, carcinogen-induced, and radiation-induced mouse sarcoma. *JCI Insight*. 2019 Jul 11;4(13). pii: 128698. doi: 10.1172/jci.insight.128698. PMID: 31112524. *equal contribution. Federal support was acknowledged (yes).

Books or other non-periodical, one-time publications. *Report any book, monograph, dissertation, abstract, or the like published as or in a separate publication, rather than a periodical or series. Include any significant publication in the proceedings of a one-time conference or in the report of a one-time study, commission, or the like. Identify for each one-time publication: author(s); title; editor; title of collection, if applicable; bibliographic information; year; type of publication (e.g., book, thesis or dissertation); status of publication (published; accepted, awaiting publication; submitted, under review; other); acknowledgement of federal support (yes/no).*

Nothing to Report

Other publications, conference papers and presentations. *Identify any other publications, conference papers and/or presentations not reported above. Specify the status of the publication as noted above. List presentations made during the last year (international, national, local societies, military meetings, etc.). Use an asterisk (*) if presentation produced a manuscript.*

- **Website(s) or other Internet site(s)**
  List the URL for any Internet site(s) that disseminates the results of the research activities. A short description of each site should be provided. It is not necessary to include the publications already specified above in this section.

The whole exome sequencing data along with the called mutations in vcf format have been deposited into the National Center for Biotechnology Information Sequence Read Archive under project ID PRJNA516973.

- **Technologies or techniques**
  Identify technologies or techniques that resulted from the research activities. Describe the technologies or techniques were shared.

  Nothing to Report

- **Inventions, patent applications, and/or licenses**
  Identify inventions, patent applications with date, and/or licenses that have resulted from the research. Submission of this information as part of an interim research performance progress report is not a substitute for any other invention reporting required under the terms and conditions of an award.

Nothing to Report

- **Other Products**

  Identify any other reportable outcomes that were developed under this project. Reportable outcomes are defined as a research result that is or relates to a product, scientific advance, or research tool that makes a meaningful contribution toward the understanding, prevention, diagnosis, prognosis, treatment and /or rehabilitation of a disease, injury or condition, or to improve the quality of life. Examples include:
  - *data or databases;*
  - *physical collections;*
  - *audio or video products;*
  - *software;*
  - *models;*
  - *educational aids or curricula;*
  - *instruments or equipment;*
  - *research material (e.g., Germplasm; cell lines, DNA probes, animal models);*
  - *clinical interventions;*
  - *new business creation; and*
  - *other.*

  Nothing to Report

7. PARTICIPANTS & OTHER COLLABORATING ORGANIZATIONS

What individuals have worked on the project?

Provide the following information for: (1) PDs/PIs; and (2) each person who has worked at least one person month per year on the project during the reporting period, regardless of the source of compensation (a person month equals approximately 160 hours of effort). If information is unchanged from a previous submission, provide the name only and indicate "no change".

Example:

Name:	*Mary Smith*
Project Role:	*Graduate Student*
Researcher Identifier (e.g. ORCID ID):	*1234567*
Nearest person month worked:	*5*
Contribution to Project:	*Ms. Smith has performed work in the area of combined error-control and constrained coding.*
Funding Support:	*The Ford Foundation (Complete only if the funding support is provided from other than this award.)*

Name:	David Kirsch MD, PhD
Project Role:	Principal Investigator
Researcher Identifier (e.g. ORCID ID):	0000-0002-2086-205X
Nearest person month worked:	1.2 CM
Contribution to Project:	Dr. Kirsch reviewed the design of all experiments and all of the data generated to complete the Aims of this proposal including histology, immunofluorescence, microscopy imaging, and flow cytometry.
Funding Support:	There is no additional funding support for this award.

Name:	Andrea Daniel, PhD
Project Role:	Research Scientist
Researcher Identifier (e.g. ORCID ID):	
Nearest person month worked:	1.08 CM
Contribution to Project:	Dr. Daniel analyzed the radiation-induced sarcomas and muscle satellite cells after radiation.
Funding Support:	There is no additional funding support for this award.

Name:	Yan Ma
Project Role:	Lab Research Analyst
Researcher Identifier (e.g. ORCID ID):	
Nearest person month worked:	5.4 CM
Contribution to Project:	Ms. Ma processes mouse tissues with formalin fixation for paraffin embedding. She performs hematoxylin and eosin staining and immunohistochemistry on the tumor sections.
Funding Support:	There is no additional funding support for this award.

Has there been a change in the active other support of the PD/PI(s) or senior/key personnel since the last reporting period?
If there is nothing significant to report during this reporting period, state "Nothing to Report."

If the active support has changed for the PD/PI(s) or senior/key personnel, then describe what the change has been. Changes may occur, for example, if a previously active grant has closed and/or if a previously pending grant is now active. Annotate this information so it is clear what has changed from the previous submission. Submission of other support information is not necessary for pending changes or for changes in the level of effort for active support reported previously. The awarding agency may require prior written approval if a change in active other support significantly impacts the effort on the project that is the subject of the project report.

Effort for the PI remains at 10% for this project as originally proposed and budgeted. For the other 90% effort, other active grants have started and ended, but these changes do not impact the effort on this project. Those projects are listed below.

AWARDED
7000000445/NNX16A069A (Fox)
Baylor College of Medicine/NASA
Mining biology's extremes for new space radiation resistance strategies

None assigned (Gersbach)
Gilbert Family Foundation
Genome Editing with Engineered Vectors to Correct Neurofibromatosis Type I

Goldman Sachs Philanthropy Fund
Emerson Collective
Dissecting the Role of Clonal Evolution in Tumor Response and Resistance to Radiation and Immunotherapy

None Assigned (Kirsch)
The Alan B. Slifka Foundation
Identifying the metabolic dependencies of primary sarcoma and sarcoma lung metastases

ENDED
5R01CA183811-04 (Alman)
NIH/NCI
Targeting Tumor Initiating Cells in Undifferentiated Pleomorphic Sarcoma

What other organizations were involved as partners?
If there is nothing significant to report during this reporting period, state "Nothing to Report."

Describe partner organizations – academic institutions, other nonprofits, industrial or commercial firms, state or local governments, schools or school systems, or other organizations (foreign or domestic) – that were involved with the project. Partner organizations may have provided financial

or in-kind support, supplied facilities or equipment, collaborated in the research, exchanged personnel, or otherwise contributed.

Provide the following information for each partnership:
Organization Name:
Location of Organization: (if foreign location list country)
Partner's contribution to the project (identify one or more)

- *Financial support;*
- *In-kind support (e.g., partner makes software, computers, equipment, etc., available to project staff);*
- *Facilities (e.g., project staff use the partner's facilities for project activities);*
- *Collaboration (e.g., partner's staff work with project staff on the project);*
- *Personnel exchanges (e.g., project staff and/or partner's staff use each other's facilities, work at each other's site); and*
- *Other.*

Nothing to Report

8. SPECIAL REPORTING REQUIREMENTS

COLLABORATIVE AWARDS: *For collaborative awards, independent reports are required from BOTH the Initiating Principal Investigator (PI) and the Collaborating/Partnering PI. A duplicative report is acceptable; however, tasks shall be clearly marked with the responsible PI and research site. A report shall be submitted to* ***https://ers.amedd.army.mil*** *for each unique award.*

QUAD CHARTS: *If applicable, the Quad Chart (available on https://www.usamraa.army.mil) should be updated and submitted with attachments.*

Not applicable.

9. APPENDICES: *Attach all appendices that contain information that supplements, clarifies or supports the text. Examples include original copies of journal articles, reprints of manuscripts and abstracts, a curriculum vitae, patent applications, study questionnaires, and surveys, etc.*

See attached revised SOW and a PDF of the following manuscript:

Lee CL*, Mowery YM*, Daniel AR*, Zhang D, Sibley AB, Delaney JR, Wisdom AJ, Qin X, Wang X, Caraballo I, Gresham J, Luo L, Van Mater D, Owzar K, Kirsch DG. Mutational landscape in genetically engineered, carcinogen-induced, and radiation-induced mouse sarcoma. *JCI Insight*. 2019 Jul 11;4(13). pii: 128698. doi: 10.1172/jci.insight.128698. PMID: 31112524. *equal contribution.

This generic Statement of Work document is intended to assist applicants with the format preferred by CDMRP. This particular SOW does not contain any specific scientific information and is intended to be easily modifiable for any project. Not all components will be applicable for every project; please consult your Program Announcement for specific award requirements.

STATEMENT OF WORK – 10/4/17
PROPOSED START DATE Aug 01, 2018
Modified 8/23/19

Site 1: Duke University
B324 LCRC
308 Research Dr.
Durham, NC 27708
PI: David Kirsch, MD, PhD

Aims	Timeline	Site 1
Major Task 1: Determine the effect of blocking p53-induced cell death on radiation-induced sarcoma	Months	
We will irradiate *CMV-rtTA; TRE-p53.1224* and littermate control C3H mouse cohorts (n=30 per sex per genotype). 3 to 4-month-old male and female mice will be placed on a dox containing diet for 10 days prior to 30 Gy to the left hind limb using a micro-irradiator (225 kVp X-rays). (Aim 1.1)	1-3	Dr. Kirsch
Mice will be examined weekly for signs of tumors. Once tumors develop, they will be harvested for histological and molecular characterization. In addition, normal (liver, muscle) tissues will be banked for future DNA sequencing experiments as a germline comparison for the radiation-induced sarcomas. (Aim 1.1)	1-24	Dr. Kirsch
Perform histology and molecular characterization of tumors by western blot and qPCR. (Aim 1.1)	18-24	Dr. Kirsch
Mice will be evaluated based on a previously published rubric for skin injury that we adapted to comprehensively assess radiation-induced normal tissue toxicity of the skin, bone, and muscle. (Aim 1.1)	1-24	Dr. Kirsch
We completed whole exome sequencing on radiation-induced sarcoma samples (months 1-12). We will perform RNAseq to search for gene expression changes that drive radiation-induced sarcomas (Aim 1.2)	12-24	Dr. Kirsch
Milestone 1: Perform statistical analysis of sarcoma-free survival of p53 wt and p53 knockdown groups and the subtypes of the radiation-induced sarcomas	24	

from each group		
Milestone 2: Determine if p53 knockdown altered the development of acute or persistent wound in response to radiation of the leg in mice	24	
Major Task 2: Dissect the mechanisms of radiation-induced sarcoma development by examining p53-dependent satellite cell fate following irradiation		
Irradiate *Pax7-nGFP; CMV-rtTA; TRE-p53.1224* mice and littermate controls and harvest muscle at 0, 1, 7, 30, 180 and 365 days following irradiation (n=5 per sex per genotype per time point). We will perform flow cytometry to determine satellite cells survival and proliferation (Aim 2.1)	3-15	Dr. Kirsch
Milestone 4: Determine if satellite cells are preserved in p53 knockdown expressing mice following irradiation	15	
Irradiate *Myf6Cre; p53$^{LSL\text{-}25,\ 26/FL}$* mice and control mice (30 mice per sex per genotype). (Aim 2.3)	4-18	Dr. Kirsch
Examine *Myf6Cre; p53$^{LSL\text{-}25,\ 26/FL}$* mice and control mice weekly for tumors and harvest tissues for histology and molecular analysis by western blot and qPCR. (Aim 2.3)	4-24	Dr. Kirsch
Milestone 6: Determine if p53 mediated cell cycle arrest and apoptosis are critical to tumor suppression in a radiation-induced sarcoma model	16	
Milestone 7: Publication of a manuscript detailing the studies in this proposal	24	

Specific Aims

1. Determine the effect of blocking p53-induced cell death on radiation-induced sarcoma.
   1.1 Evaluate the effect of blocking p53 on hind limb sarcoma development in irradiated mice

Genotype	Irradiation	Number of mice
littermate controls	None	30 female, 30 male
CMV-rtTA; TRE-p53.1224	None	30 female, 30 male
littermate controls	30 Gy left hind leg	30 female, 30 male
CMV-rtTA; TRE-p53.1224	30 Gy left hind leg	30 female, 30 male

2. Dissect the mechanisms of radiation-induced sarcoma development by examining p53-dependent satellite cell fate following irradiation.
   2.1 Test whether transient knockdown of p53 protects muscle stem (satellite) cells from radiation induced death

Genotype	Irradiation	Number of mice	Time points
Pax7-nGFP littermate controls	30 Gy left hind leg	5 female, 5 male	0, 1, 7, 30, 180, 365 Days
Pax7-nGFP; CMV-rtTA; TRE-p53.1224	30 Gy left hind leg	5 female, 5 male	0, 1, 7, 30, 180, 365 Days

   2.3 Examine the specific p53 mediated transcriptional programs necessary for tumor suppression of radiation-induced sarcoma

Genotype	Irradiated	number of mice
Myf6Cre; $p53^{-/FL}$	30 Gy left hind leg	30 female, 30 male
Myf6Cre; $p53^{+/FL}$	30 Gy left hind leg	30 female, 30 male
Myf6Cre; $p53^{LSL\text{-}25,26/FL}$	30 Gy left hind leg	30 female, 30 male
Myf6Cre; $p53^{LSL\text{-}25,26,\ 53,\ 54/FL}$	30 Gy left hind leg	30 female, 30 male

JCI insight

RESEARCH ARTICLE

Mutational landscape in genetically engineered, carcinogen-induced, and radiation-induced mouse sarcoma

Chang-Lung Lee,[1,2,3] Yvonne M. Mowery,[1,2] Andrea R. Daniel,[1] Dadong Zhang,[2] Alexander B. Sibley,[2] Joe R. Delaney,[4] Amy J. Wisdom,[5] Xiaodi Qin,[2] Xi Wang,[2] Isibel Caraballo,[1] Jeremy Gresham,[2] Lixia Luo,[1] David Van Mater,[2,6] Kouros Owzar,[2,7] and David G. Kirsch[1,2,5]

[1]Department of Radiation Oncology, [2]Duke Cancer Institute, and [3]Department of Pathology, Duke University Medical Center, Durham, North Carolina, USA. [4]Department of Biochemistry and Molecular Biology, Medical University of South Carolina, Charleston, South Carolina, USA. [5]Department of Pharmacology and Cancer Biology, [6]Department of Pediatrics, and [7]Department of Biostatistics & Bioinformatics, Duke University Medical Center, Durham, North Carolina, USA.

Cancer development is influenced by hereditary mutations, somatic mutations due to random errors in DNA replication, or external factors. It remains unclear how distinct cell-intrinsic and -extrinsic factors affect oncogenesis within the same tissue type. We investigated murine soft-tissue sarcomas generated by oncogenic alterations ($Kras^{G12D}$ activation and p53 deletion), carcinogens (3-methylcholanthrene [MCA] or ionizing radiation), and both factors in a potentially novel model (MCA plus p53 deletion). Whole-exome sequencing demonstrated distinct mutational signatures in individual sarcoma cohorts. MCA-induced sarcomas exhibited high mutational burden and predominantly G-to-T transversions, while radiation-induced sarcomas exhibited low mutational burden and a distinct genetic signature characterized by C-to-T transitions. The insertion-deletion/substitution ratio and number of gene copy number variations were high for radiation-induced sarcomas. MCA-induced tumors generated on a p53-deficient background showed the highest genomic instability. MCA-induced sarcomas harbored mutations in putative cancer driver genes that regulate MAPK signaling (*Kras* and *Nf1*) and the Hippo pathway (*Fat1* and *Fat4*). In contrast, radiation-induced sarcomas and $Kras^{G12D}$ $p53^{-/-}$ sarcomas did not harbor recurrent oncogenic mutations; rather, they exhibited amplifications of specific oncogenes: *Kras* and *Myc* in $Kras^{G12D}$ $p53^{-/-}$ sarcomas and *Met* and *Yap1* for radiation-induced sarcomas. These results reveal that different initiating events drive oncogenesis through distinct mechanisms.

Introduction

Approximately 50% of all cancer patients receive radiation therapy (1), which is a component of approximately 40% of all cancer cures (2). Although radiation is an effective cancer therapy, its use involves a small, but clinically significant, risk of developing a therapy-related malignancy (3). Radiation-associated cancers develop years later and are a particular concern for pediatric cancer patients because they may carry germline mutations in oncogenes or tumor suppressor genes and because they have many years to develop secondary cancers. Moreover, the estimated total lifetime risk of radiation-associated cancers may be higher in patients receiving modern radiation therapy techniques, such as intensity-modulated radiation therapy and image-guided radiation therapy (4, 5). When a second cancer develops after radiation exposure, it can be challenging to determine whether radiation caused the tumor.

Radiotherapy kills cells by generating unresolved double-stranded DNA breaks. For example, cells undergoing mitosis with unrepaired double-stranded DNA breaks after radiotherapy can die through mechanisms including mitotic catastrophe (6). Although radiation effectively kills proliferating cancer cells, it is a relatively weak carcinogen (3, 7). In contrast, the potent chemical carcinogen 3-methylcholanthrene (MCA) is nonlethal but acts as a mutagen to modify DNA sequences, primarily causing G-to-T transversions (8). Mutagenesis initiates a selection process that favors proliferative cells harboring activated oncogenes and inactivated tumor suppressor genes. However, mechanisms by which radiation-induced DNA damage and repair processes cause de novo cancer formation, as well as the specific types of DNA mutations and pathways modulated, remain poorly understood.

Authorship note: CLL, YMM, and ARD contributed equally to this work.

Conflict of interest: The authors have declared that no conflict of interest exists.

Submitted: March 7, 2019
Accepted: May 16, 2019
Published: July 11, 2019.

Reference information: *JCI Insight*. 2019;4(13):e128698. https://doi.org/10.1172/jci.insight.128698.

To identify mutational signatures specific to radiation-induced tumors and to gain insight into how distinct cell-intrinsic and -extrinsic factors affect cancer development within the same tissue type, we performed genomic analysis across murine soft-tissue sarcomas induced by MCA, oncogenic mutations, or ionizing radiation. Radiation-induced sarcomas were generated by focally irradiating the mouse hind limb using a single dose of 30 or 40 Gy (9). For comparison to radiation-induced sarcomas, we used an established genetically engineered mouse model of soft-tissue sarcoma in which localized delivery of Cre recombinase into the muscle of the hind limb activates oncogenic *Kras*^{G12D} and deletes both alleles of *p53* (10). In addition, we generated MCA-induced sarcomas in the hind limb of either WT or *p53*$^{fl/fl}$ mice in which both copies of *p53* were deleted by Cre recombinase.

Using these mouse models of oncogene-driven, chemical carcinogen–induced, or radiation-induced soft-tissue sarcoma, we performed whole-exome sequencing (WES) on paired tumor and normal tissue from each mouse and observed distinct facultative molecular signatures that are specific to each carcinogenic driver. Remarkably, ionizing radiation produced tumors with relatively low levels of nonsynonymous mutations, but a high frequency of somatic copy number alterations, with a preponderance of deletions and a tendency toward C-to-T and G-to-A transitions.

Results

Generation of primary murine sarcomas by oncogenic alterations, chemical carcinogens, and ionizing radiation. To investigate how cell-intrinsic and -extrinsic factors affect cancer development within the same tissue type, we generated primary murine sarcomas by using defined genetic and external insults, including mutations of Kras and p53 (Kras^{G12D} p53$^{-/-}$) (10), chemical carcinogen MCA (MCA-induced p53 WT and MCA-induced p53$^{-/-}$) (11), and ionizing radiation (IR-induced) (ref. 9; Figure 1A and Supplemental Table 1; supplemental material available online with this article; https://doi.org/10.1172/jci.insight.128698DS1). Kras^{G12D} p53$^{-/-}$ sarcomas were generated in *LSL-Kras*^{G12D} *p53*$^{fl/fl}$ mice following intramuscular delivery of adenovirus expressing Cre recombinase (Ad-Cre) (10). The median of the observed event times for the 6 mice with Kras^{G12D} p53$^{-/-}$ sarcomas for which data were available was 77 days after Ad-Cre injection. The latency of Kras^{G12D} p53$^{-/-}$ sarcomas was similar to MCA-induced p53$^{-/-}$ sarcomas, which were generated via intramuscular injection of both Ad-Cre and MCA into *p53*$^{fl/fl}$ mice (Supplemental Table 2). Compared with MCA-induced p53$^{-/-}$ and Kras^{G12D} p53$^{-/-}$ sarcomas, MCA-induced sarcomas generated in p53 WT mice had markedly longer latency (Supplemental Table 2). Notably, IR-induced sarcomas, which developed in mice with or without temporary (10-day) p53 knockdown during a single dose of 30 or 40 Gy focal irradiation (12), had the longest observed latency. The median observed event time was 449 days after radiation exposure (Supplemental Table 2). Histology demonstrated that sarcomas generated by these approaches were intermediate- to high-grade soft-tissue sarcomas (Supplemental Figure 1). Collectively, these mouse models provide a unique resource to comprehensively understand the mutational landscape across soft-tissue sarcomas generated through distinct oncogenic alterations and carcinogens.

Tumor-initiating factors dictate mutational load and signatures. To determine the mutational landscape of soft-tissue sarcomas, we performed WES on paired tumor and normal liver to identify somatic mutations that are specific to each tumor model (Supplemental Figure 2). Comparing across different sarcoma cohorts, MCA-induced sarcomas harbored the highest mutational burden (Figure 1, B and C). Both MCA-induced p53 WT and MCA-induced p53$^{-/-}$ sarcomas contain a median of more than 2000 nonsynonymous mutations per tumor (Figure 1C). IR-induced sarcomas harbored a substantially lower mutational load, with a median of 26 nonsynonymous mutations per tumor. The mutational burden of IR-induced sarcomas was similar to Kras^{G12D} p53$^{-/-}$ sarcomas (Figure 1, B and C). Notably, a single IR-induced sarcoma (S28) exhibited a disproportionally high number of mutations, of which about 15% were localized on chromosome 2 (Supplemental Figure 3). Further examination of S28 revealed mutations in multiple genes that control the DNA damage response, including *Brca1*, *Atrx*, and *Pole* (Supplemental Table 3), suggesting that defects in DNA repair and cell cycle checkpoint controls led to an accumulation of mutations in this tumor (13). Together, these results indicate that although MCA generates sarcomas by causing gene mutations, IR does not typically induce sarcomas by increasing mutational burden.

In addition to assessing the number of mutations, we examined the impact of different genetic and external insults on the distribution of sequence variants, including single-nucleotide variants (SNVs) and insertions-deletions (indels) (Figure 1D and Supplemental Figure 4). Compared with MCA-induced sarcomas and Kras^{G12D} p53$^{-/-}$ sarcomas, IR-induced sarcomas showed a higher median proportion of nonsynonymous mutations that are indels (P = 0.0003; Figure 1D). Further investigation revealed

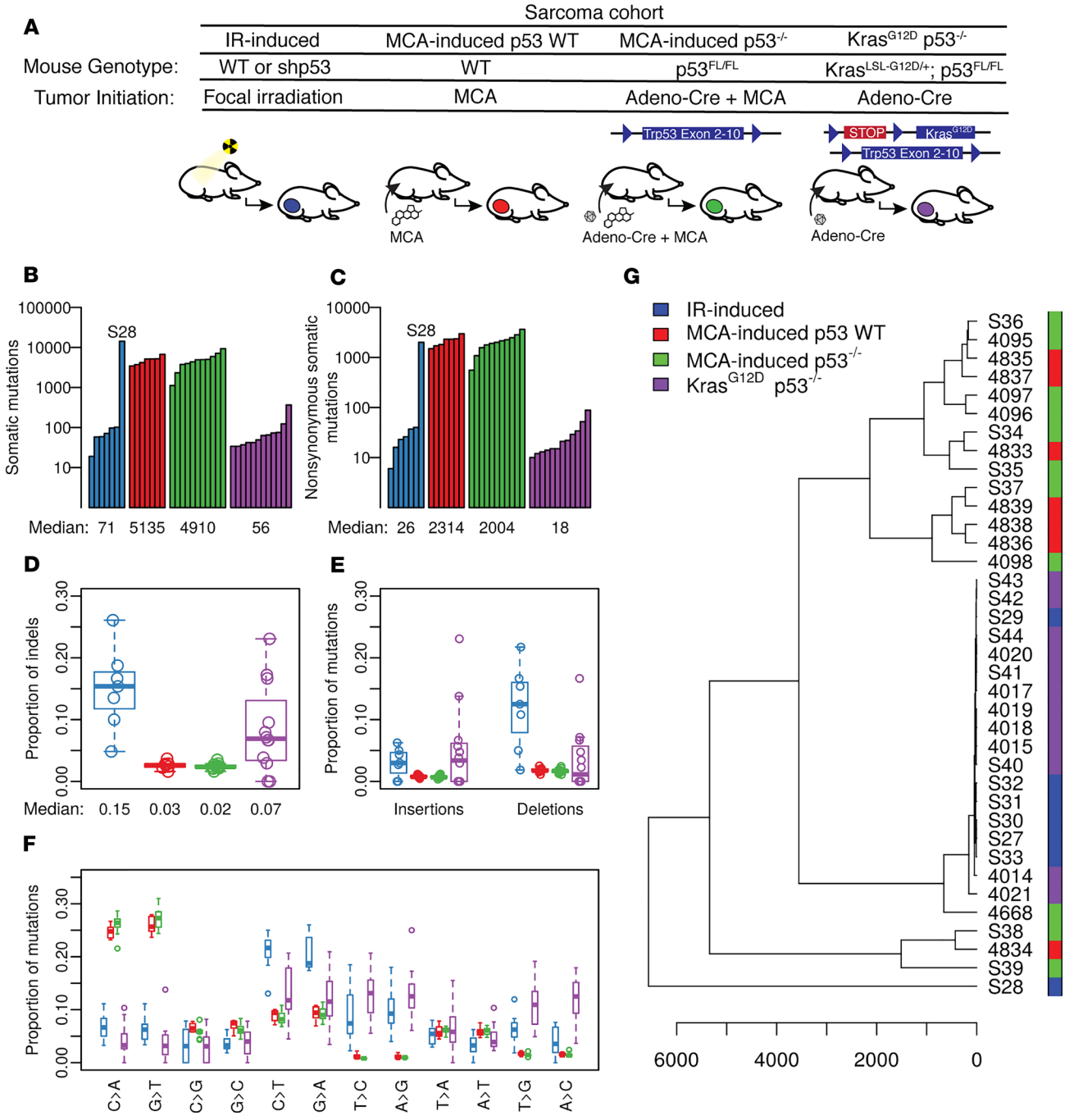

Figure 1. Somatic mutation analysis of murine soft-tissue sarcomas. (**A**) Schematics of the methods to generate various mouse models of soft-tissue sarcomas: IR-induced (blue), MCA-induced p53 WT (red), MCA-induced p53$^{-/-}$ (green), and Kras^{G12D} p53$^{-/-}$ sarcomas (purple). (**B**) The number of total somatic mutations per tumor. (**C**) The number of somatic nonsynonymous mutations per tumor. (**D**) The proportion of insertions-deletions (indels) within nonsynonymous mutations. IR-induced sarcomas showed a higher median proportion of nonsynonymous mutations that were indels (P = 0.0003). (**E**) The proportion of insertions or deletions within nonsynonymous mutations. (**F**) The proportions of different single-nucleotide substitutions. IR-induced sarcomas exhibited higher C-to-T (P = 0.0002) and G-to-A (P = 0.0006) transitions. (**G**) Unsupervised hierarchical clustering of sarcomas based on data of single-nucleotide substitutions. P values were calculated by the Kruskal-Wallis test. **B**–**G** illustrate the data for n = 37 tumors. The box plots in **D**–**F** depict the minimum and maximum values or a length of 1.5 times the interquartile range (whichever was shorter; whiskers), the upper and lower quartiles, and the median. The length of the box represents the interquartile range.

that nonsynonymous indels in IR-induced sarcomas were predominately deletions (Figure 1E). Moreover, examination of SNVs showed that although MCA-induced sarcomas harbored primarily C-to-A and G-to-T transversions, IR-induced sarcomas exhibited higher C-to-T (P = 0.0002) and G-to-A (P = 0.0006) transitions (Figure 1F). The distinction of single-nucleotide substitutions was also revealed by unsupervised hierarchical clustering showing segregation among the majority of MCA-induced sarcomas, $Kras^{G12D}$ $p53^{-/-}$ sarcomas, and IR-induced sarcomas (Figure 1G).

We further conducted signature analysis using nonnegative matrix factorization (NMF) (14), and compared our results to 30 published signatures identified in human cancers (https://cancer.sanger.ac.uk/cosmic/signatures). Our results revealed that mutational signatures derived from each murine sarcoma cohort were highly correlated with distinct Catalogue Of Somatic Mutations in Cancer (COSMIC) human signatures (Supplemental Figure 5). COSMIC signature 4, which is associated with tobacco mutagens, was exclusively enriched in MCA-induced sarcomas (Supplemental Figure 5, A and B). COSMIC signature 5, which is present universally in all 30 types of human cancers (15), was enriched in a subset of $Kras^{G12D}$ $p53^{-/-}$ sarcomas and IR-induced sarcomas. Although COSMIC signatures 9 and 17 were specifically found in certain $Kras^{G12D}$ $p53^{-/-}$ sarcomas, IR-induced sarcomas exhibited a signature that correlated with COSMIC signature 6, which may indicate microsatellite instability (Supplemental Figure 5, C and D). In sum, as shown in the mutational analysis, our results reveal unique mutational processes underlying the development of sarcomas induced by Kras and p53 mutations, MCA carcinogen, and IR.

IR and p53 status contribute to increased copy number variations. In addition to examining mutations, we evaluated somatic copy number variations (CNVs) using CODEX2 (ref. 16; Figure 2A and Supplemental Figures 2 and 6). Among sarcomas initiated in p53 WT mice, IR-induced sarcomas exhibited a markedly higher median number of genes affected by CNVs compared with MCA-induced p53 WT sarcomas (P = 0.0262; Figure 2B). This trend was consistent for both copy number gains and losses (P = 0.0262 and 0.0297; Figure 2, C and D, respectively). Moreover, MCA-induced sarcomas in p53 WT mice showed a lower median number of genes affected by CNVs compared with sarcomas initiated by MCA and p53 loss, suggesting that the p53 status of tumor cells either at the time of MCA exposure or during subsequent tumor development had a marked impact on chromosomal instability (Figure 2, B–D). $Kras^{G12D}$ $p53^{-/-}$ sarcomas, which did not develop after an external genotoxic exposure, showed a similar median number of genes with CNVs as IR-induced sarcomas (Figure 2, B–D). Together, these findings suggest that both IR and p53 loss contribute to increasing the number of CNVs during sarcomagenesis.

Different sarcoma cohorts show enrichment in genes affected by mutations versus CNVs. To elucidate genetic alterations that contribute to sarcoma development, we compared the number of genes affected by mutations versus the number affected by CNVs in each sarcoma sample. Both IR-induced sarcomas and $Kras^{G12D}$ $p53^{-/-}$ sarcomas were defined by a markedly higher number of genes affected by CNVs than mutations (Figure 3, A and B). In contrast, the majority of MCA-induced tumors exhibited relatively few genes affected by CNVs compared with mutations (Figure 3, A and B). Of note, about 50% of MCA-induced $p53^{-/-}$ sarcomas were clustered at the top right of the graph as a result of harboring both nonsynonymous SNVs and CNVs in a high number of genes (Figure 3A).

To examine genetic alterations that potentially contribute to oncogenesis, we used the COSMIC database to evaluate specific oncogenic genes that were affected by mutations and CNVs. Although the number of nonsynonymous mutations in COSMIC genes was extremely low in radiation-induced and $Kras^{G12D}$ $p53^{-/-}$ sarcomas, frequent mutations were observed in COSMIC genes in the MCA-induced tumors (Figure 3C). In contrast, the median number of COSMIC genes affected by CNVs was higher in IR-induced sarcomas, $Kras^{G12D}$ $p53^{-/-}$ sarcomas, and MCA-induced $p53^{-/-}$ sarcomas compared with MCA-induced p53 WT sarcomas (Figure 3D).

Mutations in putative driver genes of sarcomas. To evaluate putative driver genes, we analyzed recurring nonsynonymous mutations and CNVs of COSMIC genes in different sarcoma cohorts. $Kras^{G12D}$ $p53^{-/-}$ sarcomas showed essentially no recurring mutations in COSMIC genes. IR-induced sarcomas harbored recurring mutations in only 4 COSMIC genes, despite the analysis including the hypermutated sample S28 (Figure 4A). In contrast, MCA-induced sarcomas exhibited a high frequency of mutations in numerous putative driver genes, including *Kras* and *NF1* (Figure 4B). Of note, we observed p53 mutations in 100% of sarcomas (6 out of 6) that developed from p53 WT mice treated with MCA. The majority of these p53 mutations were missense mutations located in the DNA binding domain (Supplemental Figure 7). However, no p53 mutations were observed in sarcomas (0 out of 8) that developed in p53 WT mice induced by IR.

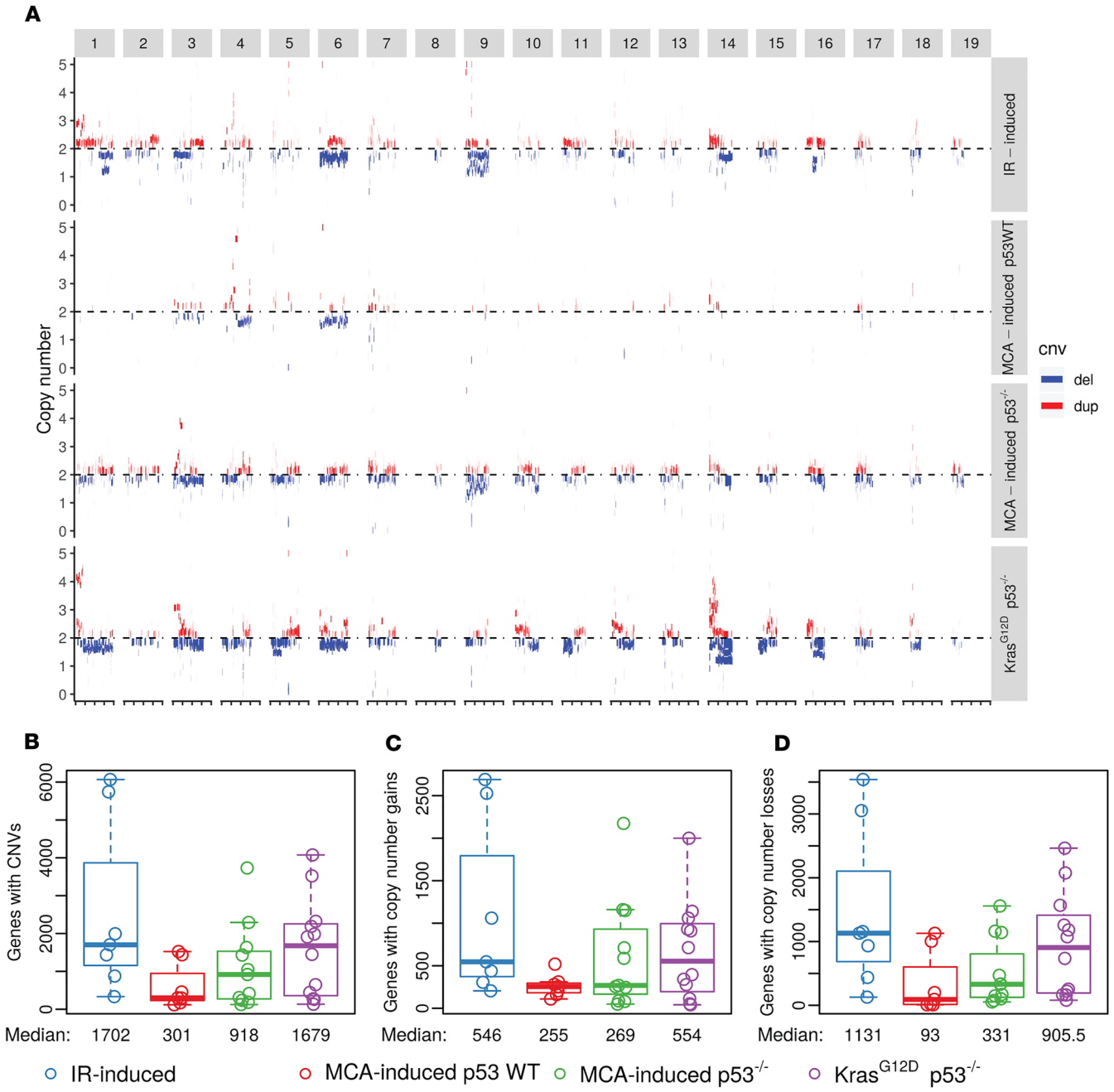

Figure 2. Somatic CNVs in mouse soft-tissue sarcomas. (**A**) Schematics of CNVs across 19 chromosomes. Results represent pooled data from sarcomas of the same cohort. DNA deletions (del) and duplications (dup) are labeled with blue and red, respectively. (**B**) The number of genes affected by CNVs. IR-induced sarcomas exhibited higher numbers of genes affected by CNVs than MCA-induced p53 WT sarcomas ($P = 0.0262$). (**C**) The number of genes with copy number gains. IR-induced sarcomas exhibited higher numbers of genes with copy number gains than MCA-induced p53 WT sarcomas ($P = 0.0262$). (**D**) The number of genes with copy number losses. IR-induced sarcomas exhibited higher numbers of genes with copy number losses than MCA-induced p53 WT sarcomas ($P = 0.297$). *P* values were calculated by the Mann-Whitney *U* test. Panels illustrate the data for $n = 37$ tumors. The box plots in **B**–**D** depict the minimum and maximum values or a length of 1.5 times the interquartile range (whichever was shorter; whiskers), the upper and lower quartiles, and the median. The length of the box represents the interquartile range.

Examination of genes affected by CNVs revealed amplification of a distinct spectrum of COSMIC oncogenes in $Kras^{G12D}$ $p53^{-/-}$ sarcomas versus IR-induced sarcomas (Figure 5A and Supplemental Tables 4–7). Although a subset of $Kras^{G12D}$ $p53^{-/-}$ sarcomas had amplifications of oncogenes *Kras* and *Myc*, several IR-induced sarcomas exhibited prominent amplifications of *Met* and *Birc3* (Figure 5A). An increase in CNVs of *Met* and *Birc3* resulted from partial amplifications of chromosomes 6 and 9, respectively (Figure 5B). The fragment that was amplified on chromosome 9 contains multiple putative driver genes, including

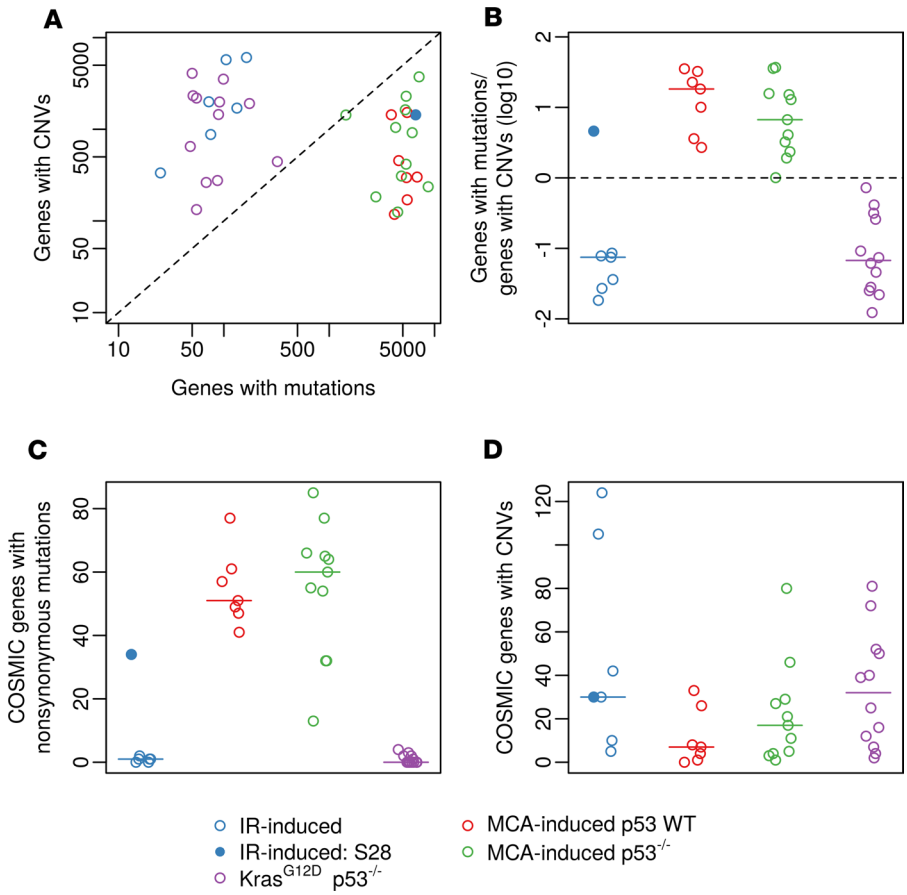

Figure 3. The relationship between somatic mutations and CNVs among sarcomas generated by discrete tumor-initiating events. (**A**) The number of genes affected by mutations versus the number of genes affected by CNVs within each sarcoma sample. (**B**) The ratio of the number of genes affected by mutations to the number of genes affected by CNVs. In panels **A** and **B**, the dashed line indicates equal numbers of mutations and CNVs. (**C**) The number of COSMIC genes affected by nonsynonymous mutations per tumor. (**D**) The number of COSMIC genes affected by CNVs per tumor. In **C** and **D**, horizontal lines indicate median values for each cohort. All panels illustrate the data for n = 37 tumors.

Yap1 (Supplemental Table 4). To validate the results from the WES data, we performed quantitative reverse transcription PCR (qRT-PCR) to examine CNVs of *Met*, *Birc3*, and *Yap1* (Figure 5C). Our results from qRT-PCR were consistent with the findings from WES, showing amplification of *Met* in IR-induced sarcomas S28, S31, and S32, as well as amplifications of *Birc3* and *Yap1* in IR-induced sarcomas S32 and S33.

Discussion

Radiation-associated sarcomas are a rare but substantial potential late side effect of radiation therapy (17). However, methods are currently lacking to discern whether a second malignancy is caused by radiation exposure. To date, a robust mutational signature for distinguishing IR-initiated cancers from tumors driven by other pathogenetic events has not been defined. Because the genetic drivers of radiation-related cancers may differ from spontaneous cancers, identifying specific genetic features in tumors that contribute to an IR signature has the potential to not only affect diagnosis but also affect therapy. Searching for a genetic signature of radiation-associated cancer in human samples is complicated by variations in radiation dose and fractionation, anatomic location, tumor type, and uncertainty regarding whether radiation initiated the tumor. In contrast, our primary murine sarcoma models provide a well-controlled system to search for a genetic signature of radiation-driven tumorigenesis. We used WES to characterize the genetic changes in sarcomas derived from 4 mouse models with distinct and clearly defined tumor-initiating events: high-dose focal IR, chemical carcinogen (MCA), p53 loss with a chemical carcinogen (MCA), and p53 loss with Kras activation.

A mutational signature depends on the mechanism of mutagenesis and subsequent selection process that malignant cells undergo during tumor development. For example, MCA metabolites form

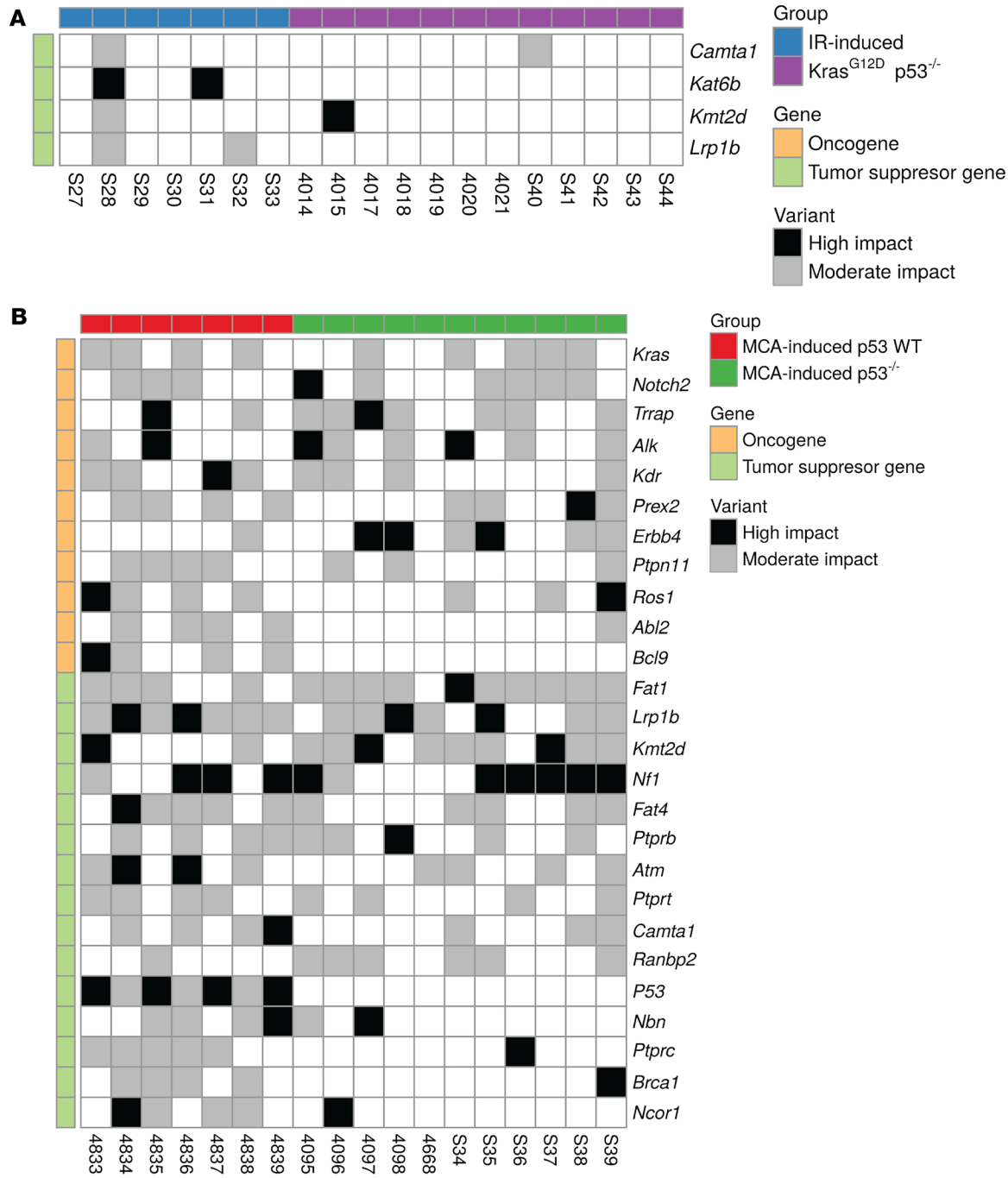

Figure 4. Nonsynonymous mutations in COSMIC genes across murine soft-tissue sarcomas. (**A**) Mutations in COSMIC genes that occurred in more than 1 IR-induced or Kras^{G12D} p53$^{-/-}$ sarcoma. (**B**) Mutations in COSMIC genes that occurred in more than 50% of MCA-induced p53 WT or MCA-induced p53$^{-/-}$ sarcomas. In both panels, genes are ordered within type by the number of samples with mutations. **A** and **B** illustrate the data for 19 and 18 tumors, respectively.

covalent bonds with double- and single-stranded DNA, preferentially at guanine residues, to produce G-to-T transversions (8). Therefore, the specific base changes that predominate in the MCA-induced p53 WT and MCA-induced p53$^{-/-}$ sarcomas are G-to-T and the reverse (C-to-A) single-base substitutions (Figure 1F). IR generates DNA damage when energy is directly absorbed by DNA molecules and indirectly through ionization of water or other intracellular molecules to generate hydroxyl radicals that cause 2-deoxyribose oxidation (18, 19). Guanine residues are particularly sensitive to oxidation compared with cytosine, thymine, and adenine, and 8-oxo-7,8-dihydro-2′-deoxyguanosine (8-oxoG) is

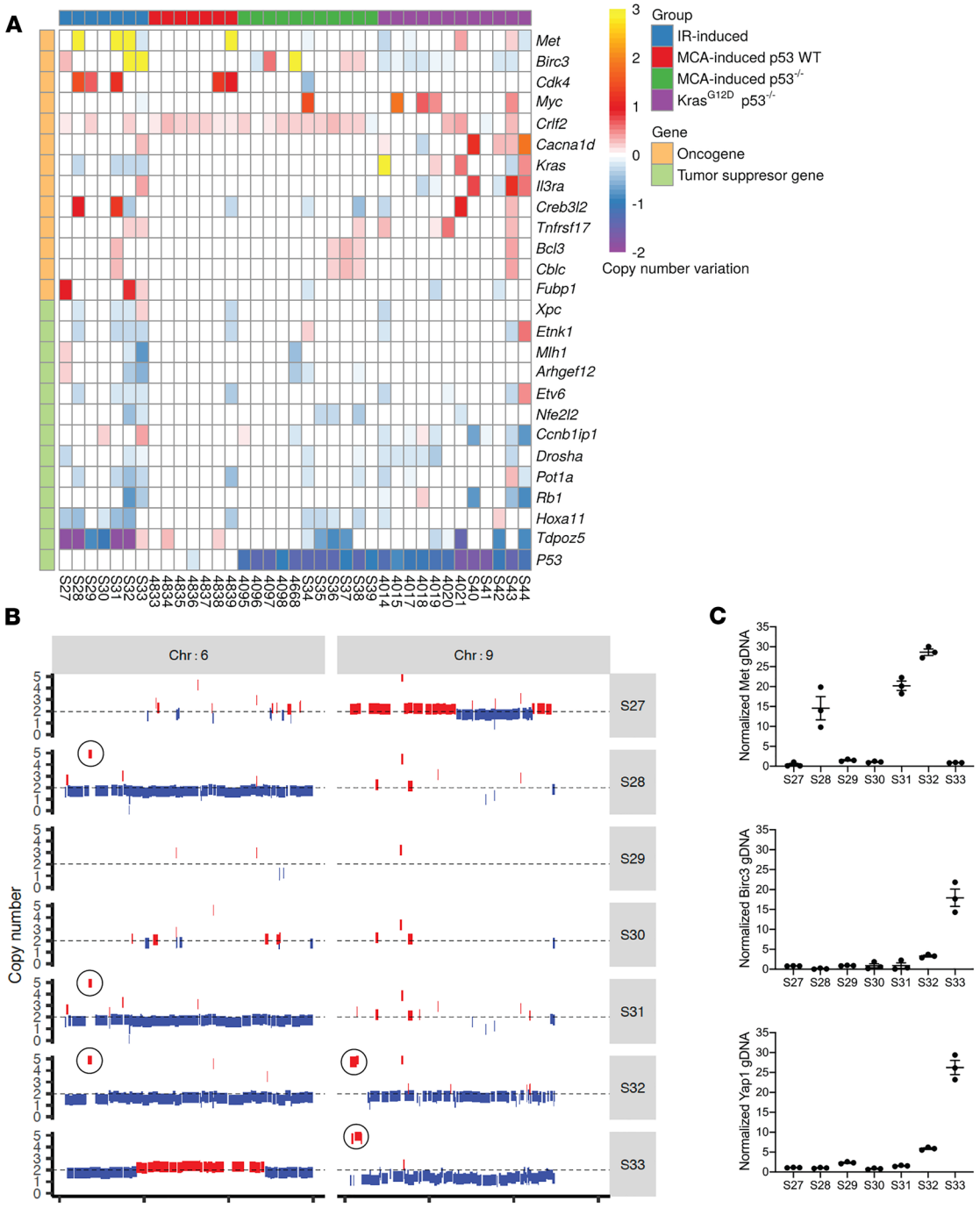

Figure 5. CNVs in COSMIC genes across murine soft-tissue sarcomas. (**A**) COSMIC oncogenes that show a mean copy number gain and COSMIC tumor suppressor genes that show a mean copy number loss in 37 murine sarcomas. Genes are ordered within gene type by mean copy number across all samples. (**B**) CNVs of chromosomes 6 and 9 of 7 IR-induced sarcomas. DNA deletions and duplications are labeled with blue and red, respectively. Circles indicate amplicons that encompass *Met* on chromosome 6 and *Birc3* on chromosome 9. (**C**) Detection of *Met*, *Birc3*, and *Yap1* DNA amplification in 7 IR-induced sarcomas by qRT-PCR. Error bars represent mean ± SEM for 3 technical replicates.

among the most readily detected base products after IR (20). Subsequently, 8-oxoG itself is far more susceptible to further oxidation, yielding more stable molecules, including spiroiminodihydantoin and guanidinohydantoin, which are more mutagenic (18). 8-oxoG adducts predominately lead to G-to-C and T-to-A transitions (21). Furthermore, reactive oxygen species through Fenton chemistry lead to deamination of methylated cytosines and thymine single-base substitutions (22, 23). Therefore, G-to-A and C-to-T DNA transition mutations are hallmarks of oxidative damage (23). Previous analyses of

radiation-associated human tumors (24, 25) and radiation-induced mouse tumors (26) reported a prevalence of C-to-T transitions. Our data, which include specific controls for alternative tumor-initiating events, demonstrate a preference for C-to-T and the reverse (G-to-A) base sequence mutations in radiation-induced tumors (Figure 1F), indicating a strong oxidative mutation signature generated by IR.

Although the single-base substitution patterns for each tumor model reveal distinguishing underlying mechanistic information, the overall somatic mutational load also provides insights into tumor initiation. MCA is a potent mutagen that generates sarcomas with roughly 80 times the median number of mutations compared with IR-induced sarcomas or $Kras^{G12D}$ $p53^{-/-}$ sarcomas (Figure 1B). Thus, the MCA-driven $p53^{-/-}$ sarcomas represent a potentially novel, spatially and temporally restricted, high–mutational load mouse model in which autochthonous tumors develop over 10–18 weeks (Supplemental Table 2), evolving under the selective pressure of an intact immune system. In contrast with conventional genetically engineered mouse models, such as the $Kras^{G12D}$ $p53^{-/-}$ sarcomas, the MCA-driven $p53^{-/-}$ sarcomas exhibit a mutational load similar to many human cancers that respond to immunotherapy (27, 28). Therefore, this model will be an important new tool to study the coevolution of tumors with the immune system and a preclinical platform to test immunotherapy.

Remarkably, the radiation-induced sarcomas exhibited relatively few nonsynonymous somatic mutations (Figure 1C). The low mutational load in the radiation-induced tumors is surprising, but this is consistent with radiation acting as a relatively weak carcinogen (3, 7). Notably, others have reported higher mutational loads in radiation-induced mouse tumors (26). Potential explanations for this discrepancy include differences in tumor types analyzed and radiation dose and fractionation. Moreover, a reference genome was used to call somatic mutations (26), which has the potential to increase the number of called mutations. In contrast, we performed WES using paired normal tissue as the reference for each tumor. Consistent with our findings, studies examining human radiation-associated tumors reported a relatively low mutational load (24, 25, 29). Because we did not sequence other tumor types or include tumors that developed after fractionated radiation exposure, the signature defined herein may not be universal for all radiation-induced cancers.

Although radiation-induced sarcomas exhibited a low number of mutations, they were composed of a higher proportion of nonsynonymous deletion events compared with $Kras^{G12D}$ $p53^{-/-}$ and MCA-driven sarcomas (Figure 1E). This result corroborates the finding from Behjati et al. (25) showing that insertions and deletions were not equally represented in human radiation-associated second malignancies, but rather that deletions were enriched and evenly distributed throughout the genome (25). Although deletions were relatively common, perhaps suggesting a loss of tumor suppressor function, none of the radiation-induced sarcomas in this study exhibited a mutation in the p53 gene. In fact, no specific driver mutations were identified in this tumor cohort (Figure 4A). However, the low mutational burden observed by WES in the mouse radiation-induced sarcomas represents a limitation for identifying specific driver mutations and conducting NMF signature analysis. In contrast, gene copy number changes were more abundant in radiation-induced sarcomas compared with $Kras^{G12D}$ $p53^{-/-}$ and MCA-driven tumors. Oncogenes *Met*, *Yap1*, and *Birc3* each exhibited copy number gains in approximately half of the radiation-induced tumors (Figure 5C). Notably, the Yap1 pathway is commonly activated in rhabdomyosarcomas, and Yap1 overexpression in muscle satellite cells is sufficient to induce sarcomagenesis in the context of muscle injury (30).

In contrast with the radiation-induced tumors, which retained WT p53 genes, all MCA-induced tumors from WT mice acquired a p53 mutation (Figure 4B and Supplemental Figure 7). Although 7 of 8 of the radiation-induced tumors arose from mice that received 10 days of doxycycline to induce p53 shRNA during radiation (i.e., temporary p53 knockdown), doxycycline was removed immediately following irradiation, and mice subsequently remained on normal chow for the remainder of the experiment. Notably, the radiation-induced tumor that arose from a mouse lacking the p53 shRNA gene likewise did not harbor a detectable p53 mutation. The MCA-induced tumors that developed on a p53 WT background exhibited increased incidence of tumor suppressor mutations compared with MCA-induced tumors that developed in the setting of Cre-mediated p53 deletion. Interestingly, the MCA-induced p53 WT tumor mutational spectrum differed substantially from that of the MCA-induced $p53^{-/-}$ tumors. The tumors that arose in WT mice with initially intact p53 developed over a longer period and activated different pathways. Indeed, oncogenes *Abl2* and *Bcl9* and tumor suppressors *Nbn*, *Ptprc*, *Brca1*, and *Ncor1* were altered in over half of the MCA-induced p53 WT tumors versus almost none of the MCA-induced $p53^{-/-}$ tumors (Figure 4B). These findings suggest that p53 mutation timing, before versus as a consequence of MCA exposure, shapes the mutational landscape by altering the selective pressure for cells to mutate specific genes. Notably, Kras

was mutated in half of all MCA-driven tumors independent of p53 status. Moreover, the tumor suppressor Fat1 was mutated in nearly all MCA tumors, and *Fat4*, *Notch2*, and *NF1* were also commonly disrupted (Figure 4B). Our study comports with sequencing data from a commonly used MCA-driven sarcoma cell line derived from immunodeficient mice ($Rag2^{-/-}$) (31). Furthermore, our comprehensive analysis of a large cohort of MCA-driven tumors supports the utility of this well-characterized primary mouse model of sarcoma for preclinical drug development studies in the presence of an intact immune system.

The genetic landscape of radiation-induced tumors reported here is distinct from published signatures for other carcinogenic processes, such as aging (32) or UV exposure (33). In studies examining radiation-associated liver tumors, higher radiation dose resulted in an increased fraction of cells harboring p53 mutations, likely through a clonal expansion mechanism (34). We previously published a report detailing the non–cell-autonomous mechanism by which radiation induces lymphomagenesis (12). In this case, total-body irradiation eliminates cells in the bone marrow niche, allowing thymic cells with preexisting oncogenic mutations to expand into a tumor unencumbered by cell competition from the bone marrow. However, the mechanisms for radiation-induced sarcomagenesis may be distinct from radiation-induced lymphomagenesis. The WES provides evidence of radiation-induced oxidative DNA damage and amplification of genes such as *Met* and *Yap1*, which are both associated with injury-induced sarcomas (35), suggesting a cell-autonomous mechanism. We suspect that after tumor-initiating cells undergo radiation-induced DNA damage, they begin clonal expansion and develop into a tumor through a selection process shaped by acute and chronically injured surrounding tissue following radiation exposure. The microenvironment of irradiated tissue is characterized by high levels of inflammatory cells and increased growth factor secretion to stimulate wound healing. Tumors that arise under these conditions are adapted to take advantage of the abundant cytokines in this milieu (36). Therefore, radiation-induced cancer may respond to different therapeutic approaches, including immunotherapy, compared with tumors from the same tissue that develop independent of radiation exposure. Defining a signature of radiation-induced cancer that can identify and characterize these tumors is a critical step toward optimizing treatment for this challenging clinical problem.

Methods

Mouse strains and sarcoma induction

To study IR-induced sarcomas, we used previously described mouse models expressing a doxycycline-inducible shRNA against p53, including *CMV-rtTA TRE-p53.1224* and *Actin-rtTA TRE-p53.1224* mice, as well as their littermates that express only *rtTA* or *TRE-p53.1224* (12). These mice were provided by Scott Lowe (Memorial Sloan Kettering Cancer Center, New York, New York, USA). All mice were on a C3H and C57BL/6J mixed genetic background. Six- to 24-week-old mice were placed on a doxycycline diet for 10 days before irradiation (12). The left hind limb of the mice was irradiated with 30 or 40 Gy, and then animals were immediately returned to normal chow. Hind limb irradiation was performed using the X-RAD 225Cx small-animal image-guided irradiator (Precision X-Ray). The irradiation field included the whole left hind limb and was defined using fluoroscopy with 40-kVp, 2.5-mA x-rays using a 2-mm aluminum filter. Irradiations were performed using parallel-opposed anterior and posterior fields with an average dose rate of 300 cGy/min prescribed to midplane with 225-kVp, 13-mA x-rays using a 0.3-mm copper filter.

Genetically engineered and carcinogen-induced primary sarcomas were generated in 6- to 10-week-old mice with a mixed genetic background. *LSL-Kras* mice were provided by Tyler Jacks (MIT, Cambridge, Massachusetts, USA) and $p53^{fl/fl}$ mice were provided by Anton Berns (Netherlands Cancer Institute, Amsterdam, The Netherlands). Primary $Kras^{G12D}$ $p53^{-/-}$ sarcomas were induced by injection of Ad-Cre (Viral Vector Core, University of Iowa, Iowa City, Iowa, USA) into the gastrocnemius of $LSL\text{-}Kras^{G12D}$ $p53^{fl/fl}$ mice (10). Carcinogen-induced sarcomas in mice with intact p53 (MCA-induced p53 WT) were generated by intramuscular injection of 300 μg MCA (MilliporeSigma) resuspended in sesame oil (MilliporeSigma) at 6 μg/μL. MCA-induced sarcomas were induced in the setting of p53 deletion by intramuscular Ad-Cre injection into the gastrocnemius of $p53^{fl/fl}$ mice (MCA-induced $p53^{-/-}$), followed 24 hours later by a 300-μg injection of MCA.

After treatment, mice were examined weekly for sarcomas. Upon detection, tumors were harvested, with half submerged in RNAlater (Thermo Fisher Scientific) for subsequent DNA isolation and half formalin-fixed for histological analysis. Livers were collected for normal tissue control samples.

WES methods

Tumor specimens and matched liver control samples stored in RNAlater were used for DNA extraction. DNA extraction was performed using DNeasy Blood and Tissue Kit or AllPrep DNA/RNA Mini Kit (Qiagen). WES was performed in 2 batches using either previously described methods (batch 1) (35) or the following method (batch 2) (Supplemental Table 1). One mouse in the $Kras^{G12D}$ $p53^{-/-}$ cohort, S45, was excluded from analyses after WES showed no evidence of a deletion of *p53* exons 2–10. Genomic DNA samples were quantified using fluorometric quantitation on the Qubit 2.0 (Thermo Fisher Scientific). For each sample, 200 ng of DNA was sheared using Focused-ultrasonicators (Covaris) to generate DNA fragments of about 300 bp in length. Sequencing libraries were then prepared using the Agilent SureSelect^{XT} Mouse All Exon Kit (S0276129). During adapter ligation, unique indexes were added to each sample. Resulting libraries were cleaned using Solid Phase Reversible Immobilization beads (Beckman Coulter) and quantified on the Qubit 2.0, and size distribution was checked on an Agilent Bioanalyzer. Libraries were subsequently enriched individually by hybridization of the prepared genomic DNA libraries with mouse all-exome target-specific probes provided with the SureSelect^{XT} Mouse All Exon Kit. The kit has a target size of 49.6 megabases. After hybridization, the targeted molecules were captured on streptavidin beads (Invitrogen). Once enriched, the libraries were pooled and sequenced on the Illumina HiSeq 2500 and Illumina HiSeq 4000 with read length of 125-bp and 150-bp paired-end sequencing protocols, respectively (Supplemental Table 8). This pooling scheme generated about 14.5 to 63.5 million reads per sample, or about 6 gigabytes of data. Once generated, sequence data were demultiplexed, and FASTQ files were generated using Bcl2Fastq2 conversion software provided by Illumina. The sequencing data along with the called mutations in vcf format have been deposited into the National Center for Biotechnology Information Sequence Read Archive under project ID PRJNA516973.

WES data analyses

Somatic mutation calling. The raw sequences were first aligned to the mouse reference genome using the BWA-MEM algorithm (v0.7.12-r1039) (37). The mouse reference genome, and SNP and indel annotation data were obtained from Sanger Institute FTP site (ftp://ftp-mouse.sanger.ac.uk/): GRCm38_68.fa (md5sum b81bcde0f9246abe84208e80049d5ba8), mgp.v5.merged.snps_all.dbSNP142.vcf.gz (md5sum e778a2cbcc05fef1fac3d4025bcfb660), mgp.v5.merged.indels.dbSNP142.normed.vcf.gz (md5sum 3ceffa10ee653ef54dc0f3524b7d9a57). Somatic mutation information was from COSMIC (38), and SNPs were annotated using SNPeff (39) and Oncotator (40). The original capture file, which had been built on GRCm37 (mm9), was lifted to GRCm38 (mm10) to match with the other reference files. The aligned bam files were preprocessed by using Picard tools (v2.8.3; http://broadinstitute.github.io/picard/faq.html), followed by somatic mutation detection using GATK3-MuTect2 (41). The impact of called mutations was evaluated using Ensembl's Variant Effect Predictor (VEP) (v91.3) (42) and visualized using R package pheatmap (43).

Somatic mutation plots. Called mutations (SNVs and indels) in GATK3-MuTect2 and annotated by VEP as having "High" or "Moderate" impact were considered "protein altering." To determine oncogenic drivers, the COSMIC database (44) was used as a consistent, community-accepted database of tumor suppressors and oncogenes (release v85). Tier 1 genes were downloaded from the Cancer Gene Census, with fusion-only genes removed, and entered into MouseMine to determine murine homologs of these oncogenes and tumor suppressor genes.

The list of protein-altering mutations was filtered to only those mutations occurring within one of the identified genes, using the Bioconductor (45) R package biomaRt (46) to determine gene locations. If a sample had more than 1 mutation within a single gene, the mutation of greatest impact was retained. For non-MCA sarcoma samples, genes mutated in 2 or more samples were included in the figures. For sarcomas induced by MCA, genes mutated in more than 50% of samples in a single tumor type were included.

Mutational signatures. Signature analysis and visualization were conducted using the method of Alexandrov et al. (14) implemented in R package maftools (v1.6.15) (47).

Copy number variation. CNV was analyzed using CODEX2 (16) and visualized using R package pheatmap (v1.0.12) (43). Segments of estimated variation were compared to gene positions using the Bioconductor (45) annotation packages TxDb.Mmusculus.UCSC.mm10.knownGene (48) and org.Mm.eg.db (49). If a gene was intersected by more than 1 segment, the estimated variation with the longest sequence overlap was retained. Genes with absolute estimated variations greater than 0.2 were considered CNVs. This threshold was determined based on the observed estimated variation of the *p53* gene in samples from *p53*-deleted sarcoma cohorts (Supplemental Figure 8). Genes with CNVs in 3 or more samples from 1 tumor cohort were included in the figures.

qRT-PCR

Relative genomic DNA levels were determined using quantitative PCR assays performed on the QuantStudio 6 Flex Real-Time PCR System with PowerUp SYBR Green Master Mix (Thermo Fisher Scientific, A25742) and specific primer sets designed within exons. Target gene quantification levels were normalized to a housekeeper gene and normal tissue DNA samples using the ΔΔCT method. Primers included *Met* DNA, forward, AATATCCTCCAAGCCGCGTA; *Met* DNA, reverse, TGATGGGGAATGCACAGACT; *Yap1* DNA, forward, CAAATGTGGACCTTGGCACA; *Yap1* DNA, reverse, CCCTCACAGACTCAGAGTGG; *Brca1* DNA, forward, CGGATGCCAAGAAGAACGAG; *Brca1* DNA, reverse, GTTCCTGTTCTCTGAGGGCT; *Birc3* DNA, forward, GGACAGTCCCATGGAGAAGC; *Birc3* DNA, reverse, CAAAGGCATGGTGCTCATCG; *36B4* DNA, forward, ACTGGTCTAGGACCCGAGAAG; and *36B4* DNA, reverse, TCAATGGTGCCTCTGGAGATT.

Immunohistochemistry

Tumor tissue was fixed in 10% neutral buffered formalin for 24 to 48 hours, preserved in 70% ethanol, and embedded in paraffin. Tissues were sectioned onto a slide and stained with hematoxylin and eosin.

Statistics

The *P* values presented were 2 sided, were the results of post hoc analyses, and were not adjusted for multiple testing. When comparing a quantitative phenotype with respect to 2 groups, the Mann-Whitney *U* test was used, whereas for 3 or more groups, the Kruskal-Wallis test was used. All inferential analyses were carried out using the R statistical environment (50) along with extension packages from the Comprehensive R Archive Network (https://cran.r-project.org/) and the Bioconductor project (45). Box-and-whisker plots presented in the figures were constructed as follows: the center line indicates the median value, the bounds represent the first and third quartiles, and the whiskers extend to either a length of 1.5 times the interquartile range past the bounds or to the most extreme data value (i.e., minimum or maximum), whichever was shorter. In box and scatter plots, each dot represents the data for 1 tumor, unless otherwise indicated. In bar plots, each bar represents the data for 1 tumor, unless otherwise indicated.

Computational considerations

The analyses were conducted with adherence to the principles of reproducible analysis using the knitr package (51) for generation of dynamic reports and Mercurial (https://www.mercurial-scm.org/) for source code management. The code for replicating the statistical analysis was made available through a public source code repository (https://bitbucket.org/dcibioinformatics/kirsch-lee-sarcoma-wes/src/default/, commit ID 13:82732a597433).

Study approval

All animal procedures for this study were approved by the Institutional Animal Care and Use Committee at Duke University, Durham, North Carolina, USA.

Author contributions

CLL, YMM, ARD, and DGK designed the study. CLL, YMM, ARD, AJW, IC, LL, and DVM performed experiments. CLL, YMM, ARD, DZ, ABS, JRD, AJW, XQ, XW, JG, DVM, KO, and DGK analyzed and interpreted data. CLL, YMM, ARD, and DGK wrote the manuscript. All authors edited and approved the manuscript.

Acknowledgments

We thank Lorraine da Silva Campos, Nerissa Williams, Yan Ma, and Kennedy Davis Brock (all Duke University Medical Center) for assisting with experiments. This work was supported by the following grants: Department of Defense (W81XWH-18-1-0162 to DGK), National Cancer Institute (R35CA197616 to DGK, K99CA212198 to CLL, and K99CA207729 to JRD), Sarcoma Alliance for Research through Collaboration (5U54CA168512-02 to DGK and YMM), Radiological Society of North America Research Resident/Fellow Grant (to YMM), Whitehead Scholar Award from Duke University School of Medicine (to CLL), National Institute of Allergy and Infectious Diseases (5U19-AI067798-13 to DGK), and the Duke Cancer Center Support Grant 5P30CA14236-44.

Address correspondence to: David G. Kirsch, Duke University Medical Center, Box 91006, Durham, North Carolina 27708, USA. Phone: 919.681.8605; Email: david.kirsch@duke.edu.

1. Moding EJ, Kastan MB, Kirsch DG. Strategies for optimizing the response of cancer and normal tissues to radiation. *Nat Rev Drug Discov*. 2013;12(7):526–542.
2. Sharma RA, et al. Clinical development of new drug-radiotherapy combinations. *Nat Rev Clin Oncol*. 2016;13(10):627–642.
3. Suit H, et al. Secondary carcinogenesis in patients treated with radiation: a review of data on radiation-induced cancers in human, non-human primate, canine and rodent subjects. *Radiat Res*. 2007;167(1):12–42.
4. Hall EJ. Intensity-modulated radiation therapy, protons, and the risk of second cancers. *Int J Radiat Oncol Biol Phys*. 2006;65(1):1–7.
5. Dracham CB, Shankar A, Madan R. Radiation induced secondary malignancies: a review article. *Radiat Oncol J*. 2018;36(2):85–94.
6. Eriksson D, Stigbrand T. Radiation-induced cell death mechanisms. *Tumour Biol*. 2010;31(4):363–372.
7. Little JB. Radiation carcinogenesis. *Carcinogenesis*. 2000;21(3):397–404.
8. Shimokado K, et al. p53 gene mutation and loss of heterozygosity of chromosome 11 in methylcholanthrene-induced mouse sarcomas. *Jpn J Cancer Res*. 1998;89(3):269–277.
9. Edmondson EF, Hunter NR, Weil MM, Mason KA. Tumor induction in mice after localized single- or fractionated-dose irradiation: differences in tumor histotype and genetic susceptibility based on dose scheduling. *Int J Radiat Oncol Biol Phys*. 2015;92(4):829–836.
10. Kirsch DG, et al. A spatially and temporally restricted mouse model of soft tissue sarcoma. *Nat Med*. 2007;13(8):992–997.
11. Prehn RT, Main JM. Immunity to methylcholanthrene-induced sarcomas. *J Natl Cancer Inst*. 1957;18(6):769–778.
12. Lee CL, et al. Acute DNA damage activates the tumour suppressor p53 to promote radiation-induced lymphoma. *Nat Commun*. 2015;6:8477.
13. Campbell BB, et al. Comprehensive analysis of hypermutation in human cancer. *Cell*. 2017;171(5):1042–1056.e10.
14. Alexandrov LB, et al. Signatures of mutational processes in human cancer. *Nature*. 2013;500(7463):415–421.
15. Alexandrov LB, et al. Clock-like mutational processes in human somatic cells. *Nat Genet*. 2015;47(12):1402–1407.
16. Jiang Y, Wang R, Urrutia E, Anastopoulos IN, Nathanson KL, Zhang NR. CODEX2: full-spectrum copy number variation detection by high-throughput DNA sequencing. *Genome Biol*. 2018;19(1):202.
17. Berrington de Gonzalez A, Kutsenko A, Rajaraman P. Sarcoma risk after radiation exposure. *Clin Sarcoma Res*. 2012;2(1):18.
18. Cui L, et al. Comparative analysis of four oxidized guanine lesions from reactions of DNA with peroxynitrite, singlet oxygen, and γ-radiation. *Chem Res Toxicol*. 2013;26(2):195–202.
19. Chan W, Chen B, Wang L, Taghizadeh K, Demott MS, Dedon PC. Quantification of the 2-deoxyribonolactone and nucleoside 5′-aldehyde products of 2-deoxyribose oxidation in DNA and cells by isotope-dilution gas chromatography mass spectrometry: differential effects of gamma-radiation and Fe^{2+}-EDTA. *J Am Chem Soc*. 2010;132(17):6145–6153.
20. Cooke MS, Evans MD, Dizdaroglu M, Lunec J. Oxidative DNA damage: mechanisms, mutation, and disease. *FASEB J*. 2003;17(10):1195–1214.
21. Yasui M, Kanemaru Y, Kamoshita N, Suzuki T, Arakawa T, Honma M. Tracing the fates of site-specifically introduced DNA adducts in the human genome. *DNA Repair (Amst)*. 2014;15:11–20.
22. Kreutzer DA, Essigmann JM. Oxidized, deaminated cytosines are a source of C → T transitions in vivo. *Proc Natl Acad Sci U S A*. 1998;95(7):3578–3582.
23. Bacolla A, Cooper DN, Vasquez KM. Mechanisms of base substitution mutagenesis in cancer genomes. *Genes (Basel)*. 2014;5(1):108–146.
24. Thibodeau BJ, et al. Mutational landscape of radiation-associated angiosarcoma of the breast. *Oncotarget*. 2018;9(11):10042–10053.
25. Behjati S, et al. Mutational signatures of ionizing radiation in second malignancies. *Nat Commun*. 2016;7:12605.
26. Sherborne AL, Davidson PR, Yu K, Nakamura AO, Rashid M, Nakamura JL. Mutational analysis of ionizing radiation induced neoplasms. *Cell Rep*. 2015;12(11):1915–1926.
27. Samstein RM, et al. Tumor mutational load predicts survival after immunotherapy across multiple cancer types. *Nat Genet*. 2019;51(2):202–206.
28. Chalmers ZR, et al. Analysis of 100,000 human cancer genomes reveals the landscape of tumor mutational burden. *Genome Med*. 2017;9(1):34.
29. López GY, et al. The genetic landscape of gliomas arising after therapeutic radiation. *Acta Neuropathol*. 2019;137(1):139–150.
30. Tremblay AM, et al. The Hippo transducer YAP1 transforms activated satellite cells and is a potent effector of embryonal rhabdomyosarcoma formation. *Cancer Cell*. 2014;26(2):273–287.
31. Matsushita H, et al. Cancer exome analysis reveals a T-cell-dependent mechanism of cancer immunoediting. *Nature*. 2012;482(7385):400–404.
32. Martincorena I, et al. Somatic mutant clones colonize the human esophagus with age. *Science*. 2018;362(6417):911–917.
33. Brash DE. UV signature mutations. *Photochem Photobiol*. 2015;91(1):15–26.
34. Iwamoto KS, Mizuno T, Tokuoka S, Mabuchi K, Seyama T. Frequency of p53 mutations in hepatocellular carcinomas from atomic bomb survivors. *J Natl Cancer Inst*. 1998;90(15):1167–1168.
35. Van Mater D, et al. Injury promotes sarcoma development in a genetically and temporally restricted manner. *JCI Insight*. 2018;3(20):e123687.
36. Nguyen DH, et al. Radiation acts on the microenvironment to affect breast carcinogenesis by distinct mechanisms that decrease cancer latency and affect tumor type. *Cancer Cell*. 2011;19(5):640–651.
37. Li H. Aligning sequence reads, clone sequences assembly contigs with BWA-MEM. Cornell University. https://arxiv.org/abs/1303.3997. Published March 16, 2013. Updated May 26, 2013. Accessed June 5, 2019.
38. Forbes SA, et al. COSMIC: exploring the world's knowledge of somatic mutations in human cancer. *Nucleic Acids Res*.

2015;43(Database issue):D805–D811.
39. Cingolani P, et al. A program for annotating and predicting the effects of single nucleotide polymorphisms, SnpEff: SNPs in the genome of Drosophila melanogaster strain w1118; iso-2; iso-3. *Fly (Austin)*. 2012;6(2):80–92.
40. Ramos AH, et al. Oncotator: cancer variant annotation tool. *Hum Mutat*. 2015;36(4):E2423–E2429.
41. McKenna A, et al. The Genome Analysis Toolkit: a MapReduce framework for analyzing next-generation DNA sequencing data. *Genome Res*. 2010;20(9):1297–1303.
42. McLaren W, et al. The Ensembl Variant Effect Predictor. *Genome Biol*. 2016;17(1):122.
43. Kolde R. 2015. pheatmap: Pretty Heatmaps. R package version 1.0.8. https://CRAN.R-project.org/package=pheatmap.
44. Forbes SA, et al. COSMIC: somatic cancer genetics at high-resolution. *Nucleic Acids Res*. 2017;45(D1):D777–D783.
45. Gentleman RC, et al. Bioconductor: open software development for computational biology and bioinformatics. *Genome Biol*. 2004;5(10):R80.
46. Durinck S, Spellman PT, Birney E, Huber W. Mapping identifiers for the integration of genomic datasets with the R/Bioconductor package biomaRt. *Nat Protoc*. 2009;4(8):1184–1191.
47. Mayakonda A, Koeffler HP. Maftools: Efficient analysis, visualization and summarization of MAF files from large-scale cohor tbased cancer studies. bioRxiv. https://doi.org/10.1101/052662. Published May 11, 2016. Accessed June 5, 2019.
48. Team BC, Maintainer BP. TxDb.Mmusculus.UCSC.mm10.knownGene: Annotation package for TxDb object(s). R package version 3.4.7. Bioconductor. https://doi.org/10.18129/B9.bioc.TxDb.Mmusculus.UCSC.mm10.knownGene. Accessed June 5, 2019.
49. Carlson M. org.Mm.eg.db: Genome wide annotation for Mouse. R package version 3.8.2. Bioconductor. https://doi.org/10.18129/B9.bioc.org.Mm.eg.db. Accessed June 5, 2019.
50. R Core Team. R: A language and environment for statistical computing. R Foundation for Statistical Computing, Vienna, Austria. http://www.R-project.org/. Accessed June 5, 2019.
51. Xie Y. *Dynamic Documents with R and knitr*. Boca Raton, Florida, USA: Chapman and Hall/CRC; 2015.